Chapter 2

Synthesis and applications of 3,7-disubstituted chromen-2-one derivatives as anticancer agent

2.1 Introduction

Cancer is one of the dreadful diseases after cardiovascular diseases and diabetes falling under category of non-communicable diseases all over the world. According to WHO, more than 13 million deaths due to cancer will happen in 2030 [1]. Cancer is caused due to uncontrolled growth of cells without differentiation because of deregulation in essential enzymes and other proteins controlling cell division and proliferation [2-3]. Chemotherapy shows significant clinical responses amongst other therapeutic strategies. To get selective chemotherapeutics with very low side effects is a major challenge for treatment of cancer. These chemotherapeutic agents have a small therapeutic window with non-specificity and high-systemic toxicity [4]. Other major concern after target selectivity in chemotherapy is drug resistance to many anticancer agents. These have resulted in drug-induced toxicities and requirement of high doses of chemotherapeutic agents [5-7]. Therefore, there is need of discovering new anticancer agents with high potency for treatment of cancer [8]. Due to the potential applications of chromen-2-ones in medicinal chemistry, many efforts have been made on the design and synthesis of new chromen-2-one derivatives with improved biological activities. Chromen-2-ones exhibited antitumor activities at different stages of cancer formation through various mechanisms, for example blocking cell cycle, inducing cell apoptosis, modulating estrogen receptor (ER), or inhibiting the DNA-associated enzymes, such as topoisomerase [9]. Most of the anticancer drugs including 5-flourouracil, tamoxifen and paclitaxel exert their cytotoxicity towards cancer cell by elevating cellular Reactive oxygen species (ROS) production to a threshold level and this elevated ROS causes DNA damage and activate apoptotic pathway in cell [10-12]. Chromen-2-one derivatives containing a substituted hydroxyl group on 7^{th} position showed antibiotic and antifungal activities, while 7-hydroxy chromen-2-one derivatives showed very good cytotoxicity and cytostatic activity [13].

To counterbalance the effect of ROS, cells have antioxidant defense system which combats the effect of increased ROS in cell. Thus, the presence of antioxidant eradicates the anticancer effect of an anticancer drug which mostly exerts its effect by mean of ROS. Therefore, a potent anticancer drug should have low antioxidant property. Thus, screening of antioxidant activity provides useful insight into the mechanism of action of anticancer activity. Anticancer drugs have traditionally been targeted to damage aberrantly dividing cells by interrupting the cell division process. Some of them are DNA intercalating agents or DNA cross linking agents. Chromen-2-ones form interstrand as well as intrastrand cross linkages

and act as intercalating agents [14-15].

Recent studies on a variety of synthetic chromen-2-one derivatives have demonstrated the influence of the chromen-2-one skeleton and substitutions at 3rd and 7th positions on antitumor activities [16]. Maciejewska et al reported series of O-aminoalkyl substituted 7-hydroxy chromen-2-ones with anticancer activity [17]. Compound **1** showed good activity against various cancer cell lines such as leukemia CCRF-CEM, non-small cell lung cancer HOP-92 and colon cancer HCC-2998. Antioxidant compounds play important role in biological system by removal of free radicals generated in body. Synthetic antioxidant compounds are showing toxicity and mutagenic effects. Several chromen-2-one derivatives are reported with antioxidant activity. The applications of chromen-2-one derivatives in anticancer therapy comprise of useful source of new anticancer agents but the details of the relationship between the structure and biological activity is still to be fully understood. Recently, El-Hameed Hassan et al reported 7-hydroxy chromen-2-one derivative **2** (**Fig-2.1**) as very good antioxidant in DPPH assay with IC_{50} value 213 mg/mL [18]. W. Yubin et al reported synthesis and in vitro evaluation of novel 3, 7-disubstituted chromen-2-one derivatives as potent anticancer agents (**Figure-2.1**, compound **3**) [19].

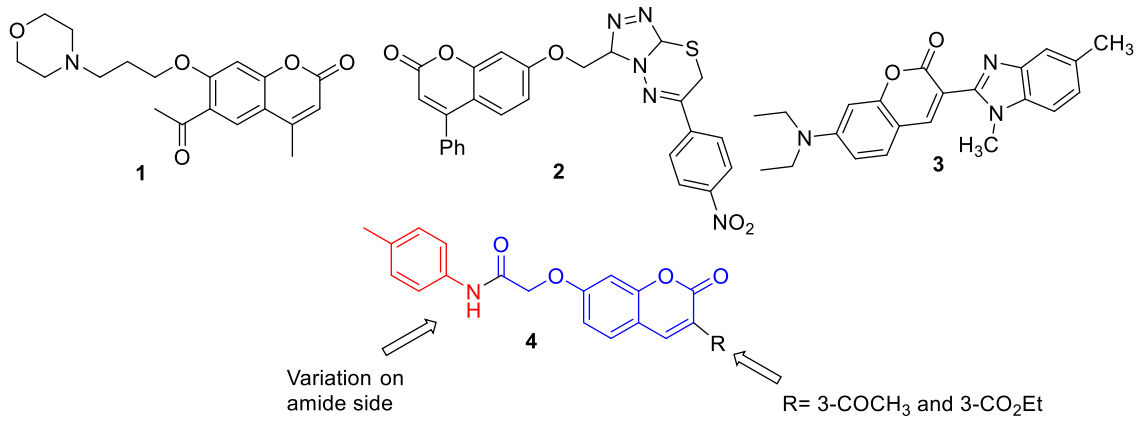

Figure-2.1 Chromen-2-one derivatives with anticancer activity.

However, there are limited reports on interactions for 3,7-disubstituted Chromen-2-ones with DNA binding studies. Based on the above literature search we have designed and synthesized 3,7-disubstituted chromen-2-ones as shown in compound **4** (**Fig-2.1**) and screened for anticancer activity by MTT assay. UV based DNA binding studies and Antioxidant activity of selected compounds was performed by DPPH assay.

2.2 Results and Discussion

2.2.1 Chemistry

Knoevenagel Reaction of 2,4-dihydroxy benzaldehyde **5** with ethyl acetoacetate gave 3-acetyl-7-hydroxy chromen-2-one **6** as shown in **Scheme-1**. The ^{1}H-NMR of compound **6** (**Fig-2.3.1**) showed singlet for three protons of methyl group at δ 2.53. Aromatic protons at position 5, 6 and 8 were observed in the range of δ 6.72-7.79, the 4th position proton observed at δ 8.56. The –OH proton observed at δ 11.14 ppm. In ^{13}C-NMR of compound **6** (**Fig-2.3.2**), the –CH_3 carbon was observed at δ 30, all aromatic carbons were observed between δ 102-159 and the lactone carbonyl carbon observed at δ 165 and ketone carbonyl carbon observed at δ 195, thus confirmed the formation of compound **6**.

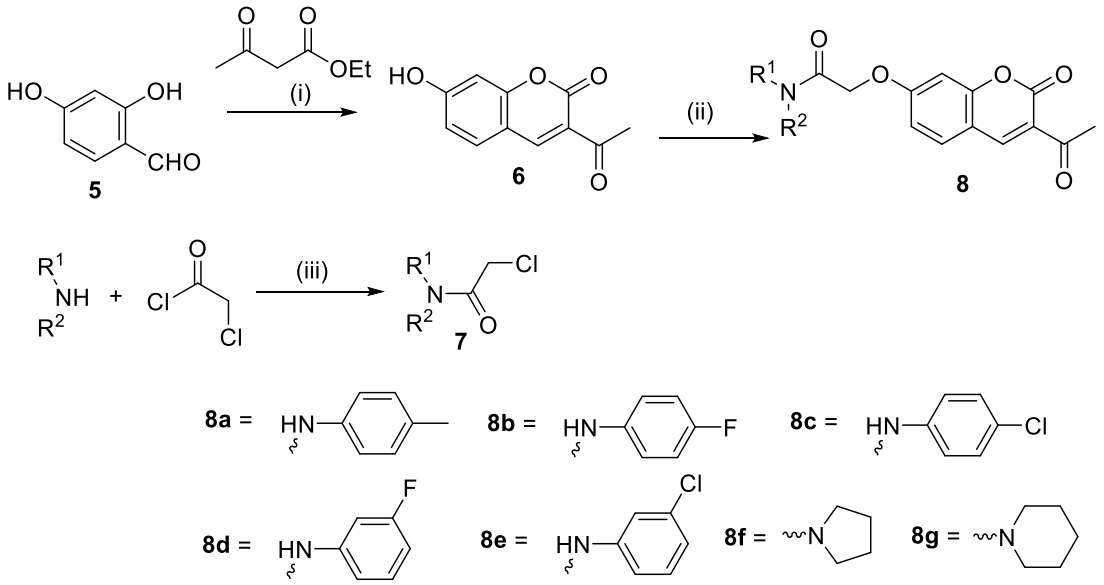

Reagents and conditions: (i) Piperidine catalytic, pyridine, bulb oven (100 W), 70-80 ^{o}C, 14 h, 74-87 %; (ii) 7, anhydrous K_2CO_3, KI pinch, DMF, 70-80 ^{o}C, 12-18 h, 43-91%; (iii) TEA, DCM, 0-5 ^{o}C, 30 min, rt, 24 h, 85-95%.

Scheme-1 Synthesis of 3-acetyl-7-disubstituted chromen-2-one derivatives 8a-g.

Chloroacetyl chloride on reaction with various amines gave substituted chloroacetamide derivatives 7. The reaction of 3-acetyl-7-hydroxy chromen-2-one 6 with various substituted chloroacetamides 7 in K_2CO_3 and DMF at 70-80 ^{o}C in presence of catalytic amount of KI gave compounds 8a-g. The structures of all 3,7-disubstituted chromen-2-one derivatives were confirmed by different spectral techniques such as ^{1}H-NMR, ^{13}C-NMR, IR, ESI-Mass.

In general, the IR spectra of compounds 8a-g exhibited three strong bands in the range of 1723-1734 cm^{-1} for lactone, 1681-1698 cm^{-1} for ketone and 1611-1670 cm^{-1} for amide carbonyl stretching frequencies. The -NH stretching frequency observed at 3340-3375 cm^{-1}.

In ^{1}H-NMR spectrum of compound 8e, the singlet for methyl three protons is observed at δ 2.55. The singlet for methylene two protons is observed at δ 4.91. All aromatic protons observed in the range of δ 7.09-8.62. The –NH proton observed at δ 10.38 (Fig-2.9.2), which was further confirmed by D_2O exchange and showed disappearance of peak at δ 10.38 (Fig-2.9.3).

In ^{13}C-NMR of compound 8e (Fig-2.9.4) the -CH_3 carbon observed at δ 30, the methylene carbon observed at δ 67ppm. All the aromatic carbons observed between δ 102-164 ppm, lactone carbonyl carbon observed at δ 166 and ketone carbonyl carbon observed at δ 195 ppm. The ESI-Mass spectrum of 8e showed M+Na peak at 393.95 (Fig-2.9.5).

In IR spectra of compounds 8f and 8g where amines used are cyclic secondary amines, the band at 3370 cm^{-1} is not observed for -NH stretching vibrations. In ^{1}H-NMR spectra of 8f and 8g showed many peaks in aliphatic region due to presence of pyrrolidine and piperidine ring (Fig-2.10.2-2.11.2).

In general for ^{1}H-NMR of compounds 8a-g peak for three methyl protons of acetyl group observed in the range of δ 2.55-2.73 ppm, methylene protons observed in the range of δ 4.71-4.92, all aromatic protons observed in the range of δ 6.82-8.66 depending on the effect of different amines. For compound 8a the -NH proton observed at δ 8.1, for all other compounds 8b-e the -NH protons observed in the range of δ 10.25-10.41 ppm. In ^{13}C-NMR spectra of compounds 8a-g, the methyl carbon of acetyl group observed at δ 30, the methylene carbon observed at δ 67 ppm, all aromatic carbons observed in the range of δ 101-161 ppm, lactone carbonyl carbon observed in the range of 163-166 ppm and ketone carbonyl carbon observed around δ 195 ppm.

Knoevenagel reaction of 2,4-dihydroxy benzaldehyde with diethyl malonate gave ethyl-3-carboxylate-7-hydroxy chromen-2-one 9 (Scheme-2). In ^{1}H-NMR of compound 9 (Fig-2.4.1) the ethyl protons of ester group observed as triplet for three protons at δ 1.29 and quartet for two protons at δ 4.25, with coupling constant 7.2 Hz. All aromatic protons at C-5, C-6 and C-8 observed in the range δ 6.73-7.77. The 4th position proton observed at δ 8.68, the -OH proton observed quite downfield at δ 11.11 ppm.

The reaction of compound 9 with various substituted chloroacetamides 7 in anhydrous K_2CO_3 and dimethyl formamide (DMF) with catalytic amount of KI at 70-80 ^{o}C gave compounds 10a-d. The structures of all compounds were confirmed by its IR, ^{1}H-NMR, ^{13}C-NMR, ESI-Mass spectra and X-ray single crystal study.

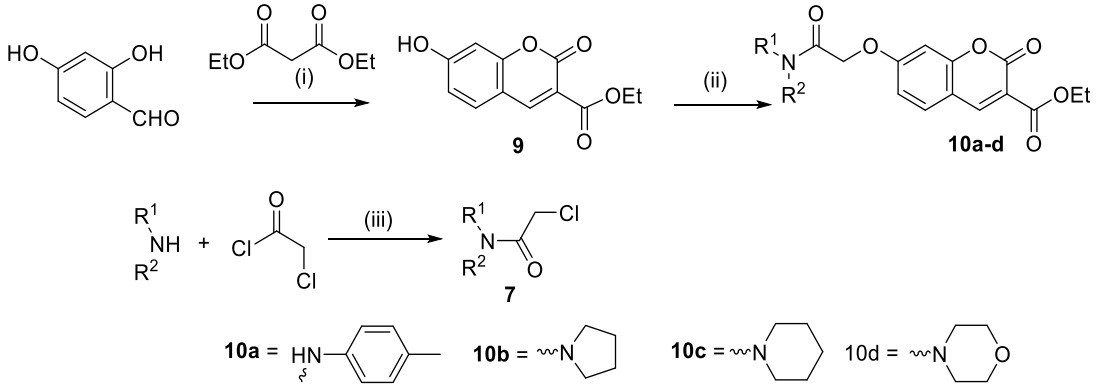

Reagents and conditions: (i) Piperidine catalytic, pyridine, bulb oven (100 W), 70-80 ^{o}C, 14 h, 74-87 %; (ii) 7, anhydrous K_2CO_3, KI pinch, DMF, 70-80 ^{o}C, 12-18 h, 43-91%; (iii) TEA, DCM, 0-5 ^{o}C, 30 min, rt, 24 h, 85-95%.

Scheme-2 Synthesis of 3-carboxylate-7-disubstituted chromene derivatives **10a-d**.

In IR spectra of **10a**, three bands are observed for carbonyl stretching frequencies of lactone carbonyl, ester carbonyl, and amide carbonyl at 1757 cm^{-1}, 1708 cm^{-1} and 1605 cm^{-1} respectively. The -NH stretching frequency observed at 3340 cm^{-1} (**Fig-2.12.1**). In ^{1}H-NMR spectrum of **10a** (**Fig-2.12.2**) the ethyl protons are observed as triplet for three protons at δ 1.42 and quartet for two protons at δ 4.42. The singlet for two protons of methylene observed at δ 4.71, all aromatic protons observed in range of δ 6.94-8.53. The -NH proton observed at δ 8.15 ppm, which was confirmed by D_2O exchange study (**Fig-2.12.3**). In ^{13}C-NMR spectrum of compound 10a showed two methyl carbons at δ 14 and 20, two -CH_2 carbons at δ 62 and 68 ppm. All aromatic carbons observed in the range of δ 102-157. The amide carbonyl carbon, ester carbonyl carbon and lactone carbonyl carbons are observed at δ 162, 163 and 164 ppm respectively (**Fig-2.12.4**). The ESI-Mass of 10a showed M+H peak at 382.05 (**Fig-2.12.5**).

For compounds **10a-d,** the IR spectra exhibited three strong bands in range of 1742-1757cm^{-1}, 1647-1708 cm^{-1} and 1602-1623 cm^{-1} for the lactone, ester and amide carbonyls respectively. In the ^{1}H NMR spectra of **10a-d**, peak for methyl protons of ester group on 3rd position of chromen-2-one observed in range of δ ~1.30-1.42 as a triplet and methylene protons observed in range of δ ~4.27-4.42 as a quartet. Protons for methylene linkage are observed in range of 4.71-5.02 and aromatic protons observed in range of 6.82-8.72 depending on effect of different substitutions on amine. In the ^{13}C-NMR spectra of **10b-d**, carbon for methyl group observed around 14 ppm, methylene carbons were observed at δ 61 and 67 ppm. For compound **10a-d**, methylene linkage carbon observed around 66-67 ppm, all aromatic carbons in range of 101-157 ppm, amide carbonyl carbon in range of 161-163 ppm, lactone

carbonyl carbon in range of 163-164 ppm and ester carbonyl carbon at 165 ppm. All compounds **8a-g** and **10a-d** were analyzed by ESI-MS analysis which showed $[M+H]^+/[M+Na]^+$ peak corresponding to their molecular weight. Structure of compound **10d** was confirmed by X-ray single crystal analysis (**Fig-2.2**) (**CCDC 1522100**) the values are given in **Table-2.1**.

All the newly synthesized compounds **8a-g** and **10a-d** were screened for their *In-Vitro* studies for anticancer activity by MTT assay method, DNA binding studies by UV spectra and antioxidant activity by DPPH assay method.

Figure-2.2: Single crystal analysis for compound **10d (**CCDC 1522100**)**

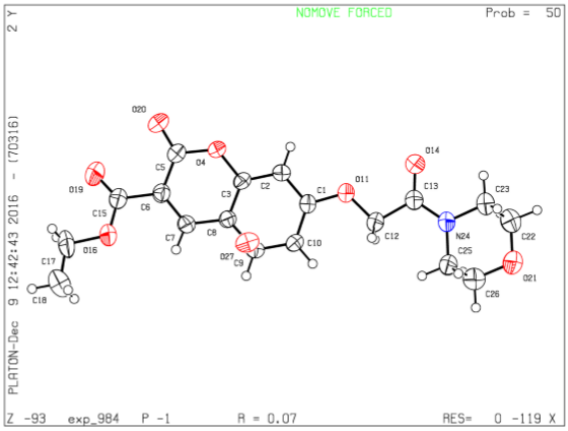

Table-2.1

Chemical formula	$C_{18}H_{19}NO_7$		ρ_{calc}mg/mm^3	1.395
Molecular weight	361		Θ	6.18 to 57.86°
Crystal system	triclinic		H	-9-8
Space group	P -1		k	-11-11
a/Å	6.9140(6)		L	-21-19
b/Å	8.3284(8)		Total reflections	6841
c/Å	16.3463(12)		Independent reflections	4033
α/°	89.585(7)		Used no. of reflections	4033
β/°	83.793(7)		R^a	0.0658
γ/°	73.740(8)		Absorption coefficient (m Å^{-1})	0.097
V/Å^3	898.05(14)		R_{int}	0.0177
Z	2		Peak and hole	0.43 and -0.30 Å Å^3

Figure-2.3.1 ^{1}H-NMR spectrum of 3-acetyl-7-hydroxy-2H-chromen-2-one (**6**) in DMSO-d_6

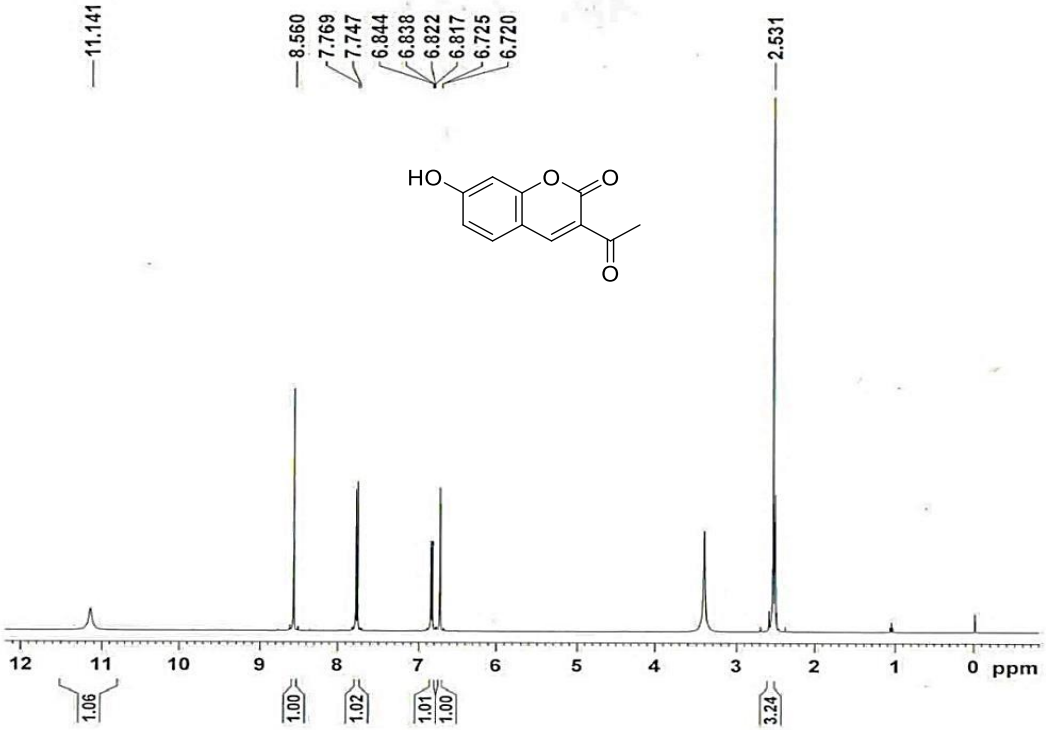

Figure-2.3.2 ^{13}C-NMR spectrum of 3-acetyl-7-hydroxy-2H-chromen-2-one (**6**) in DMSO-d_6

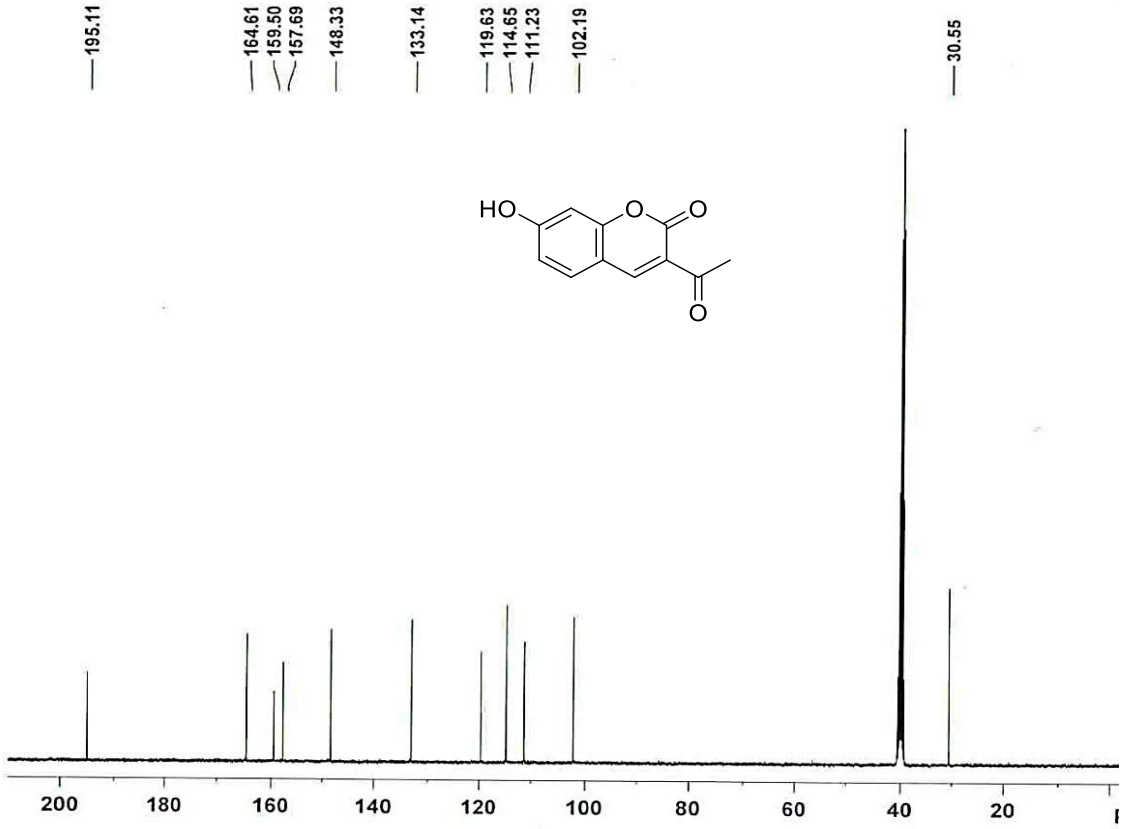

Figure-2.4.1 ^{1}H-NMR spectrum of ethyl 7-hydroxy-2-oxo-2H-chromene-3-carboxylate (**9**) in DMSO-d_6

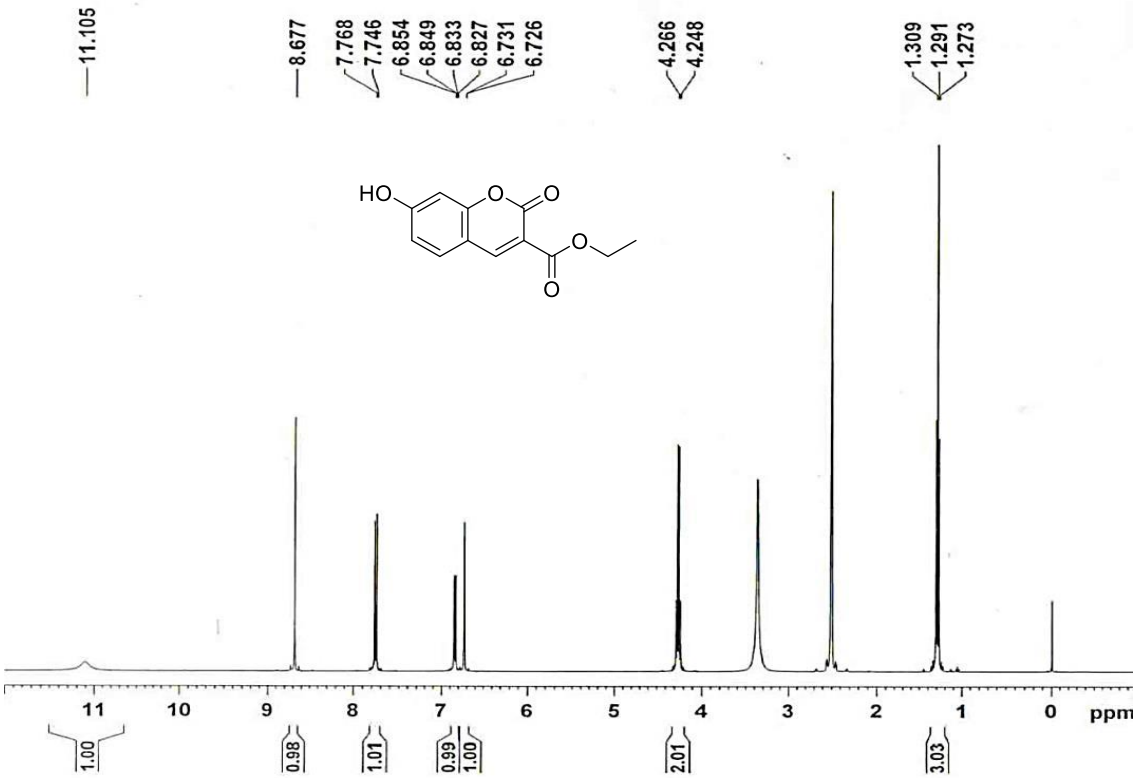

Figure-2.4.2 ^{13}C-NMR spectrum of ethyl 7-hydroxy-2-oxo-2H-chromene-3-carboxylate (**9**) in DMSO-d_6

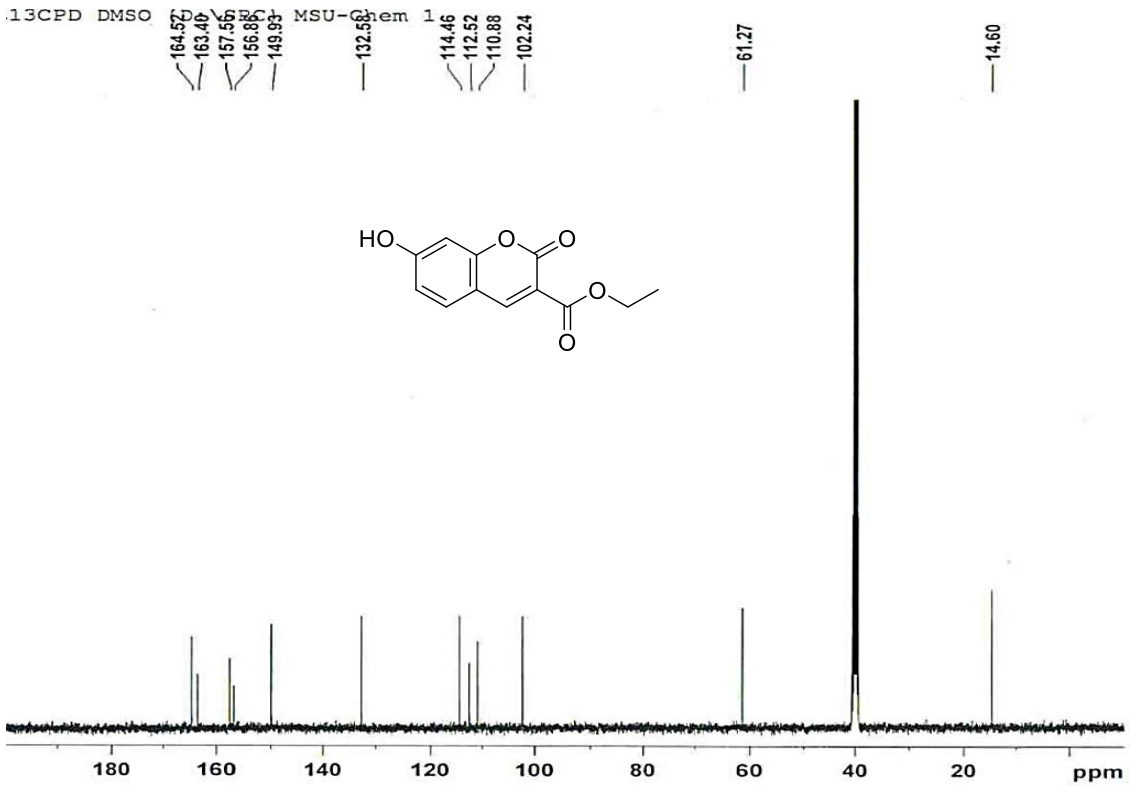

Figure-2.5.1 IR spectrum of 2-[(3-acetyl-2-oxo-2H-chromen-7-yl)oxy]-N-(4-methylphenyl)acetamide (**8a**)

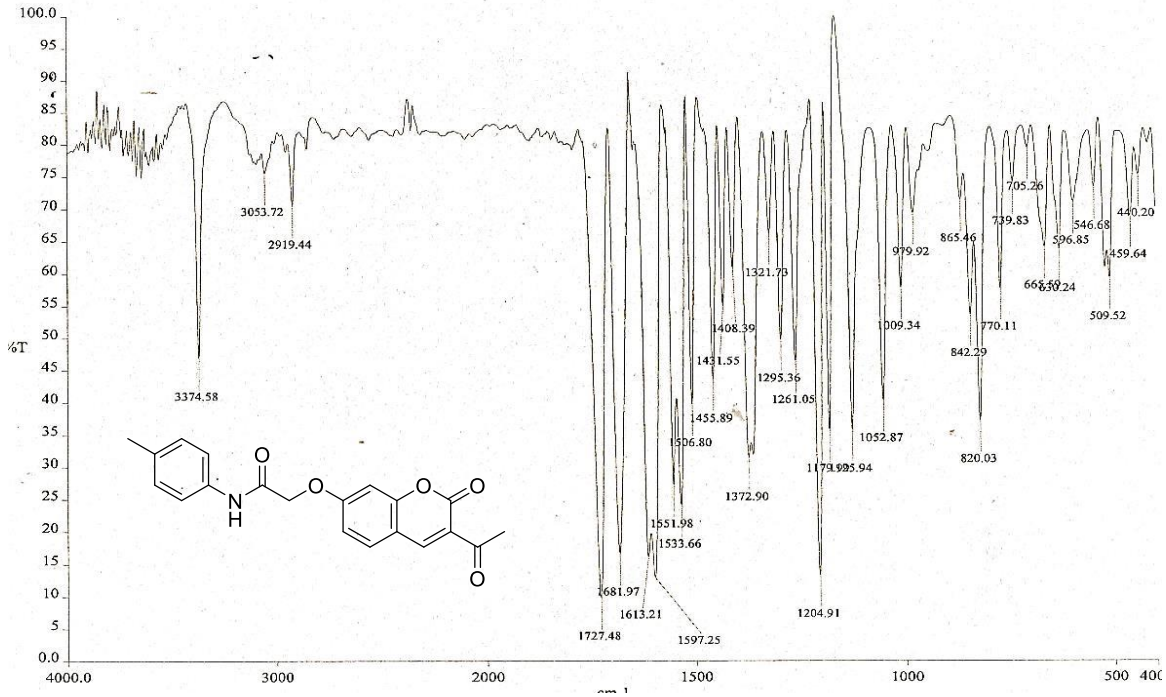

Figure-2.5.2 ^{1}H-NMR spectrum of 2-[(3-acetyl-2-oxo-2H-chromen-7-yl)oxy]-N-(4-methylphenyl)acetamide (**8a**) in $CDCl_3$

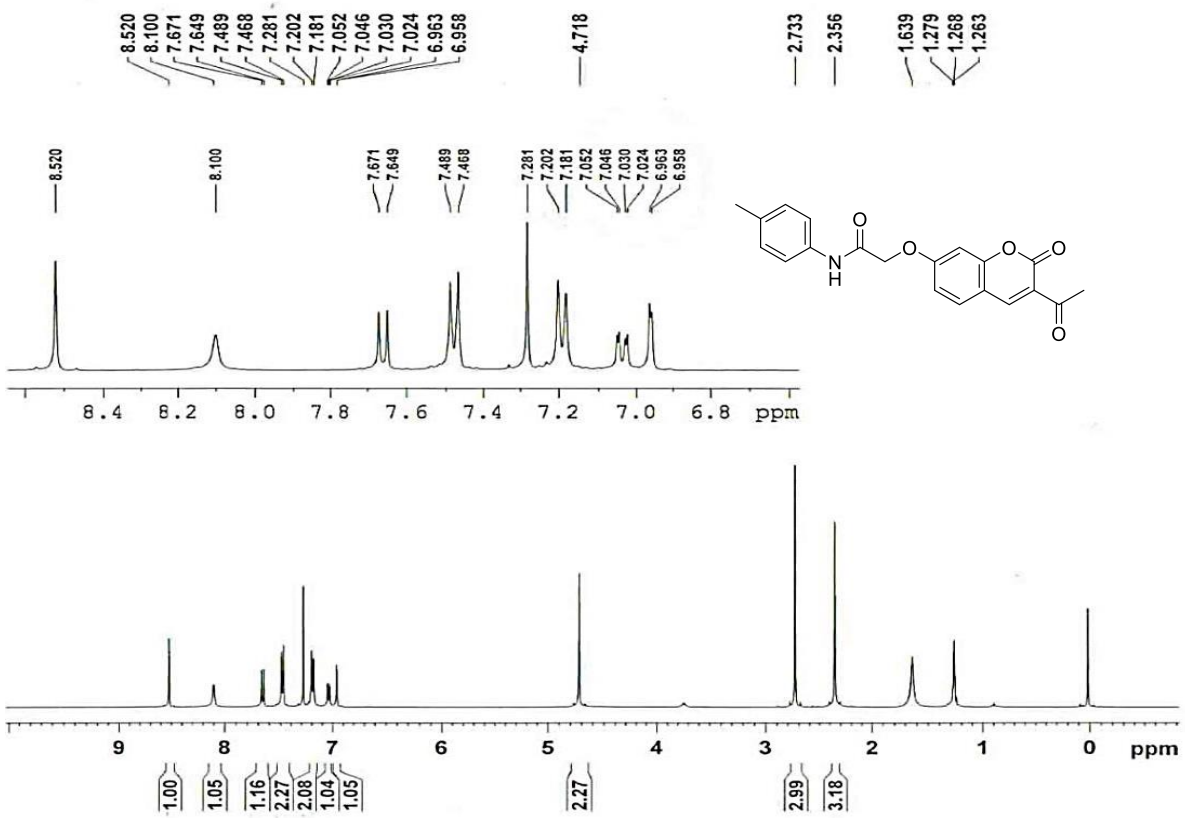

Figure-2.5.3 ^{13}C-NMR spectrum of 2-[(3-acetyl-2-oxo-2H-chromen-7-yl)oxy]-N-(4-metyhlphenyl)acetamide (**8a**) in $CDCl_3$

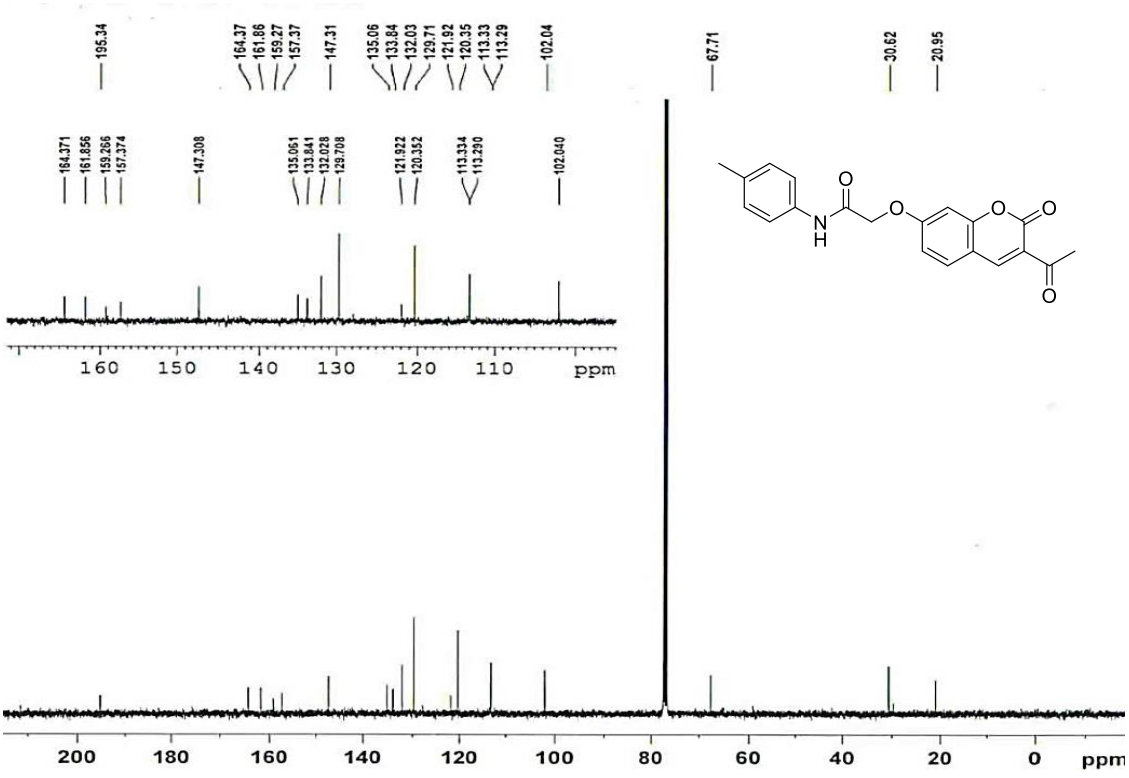

Figure-2.6.1 IR spectrum of 2-[(3-acetyl-2-oxo-2H-chromen-7-yl)oxy]-N-(4-fluorophenyl)acetamide (**8b**)

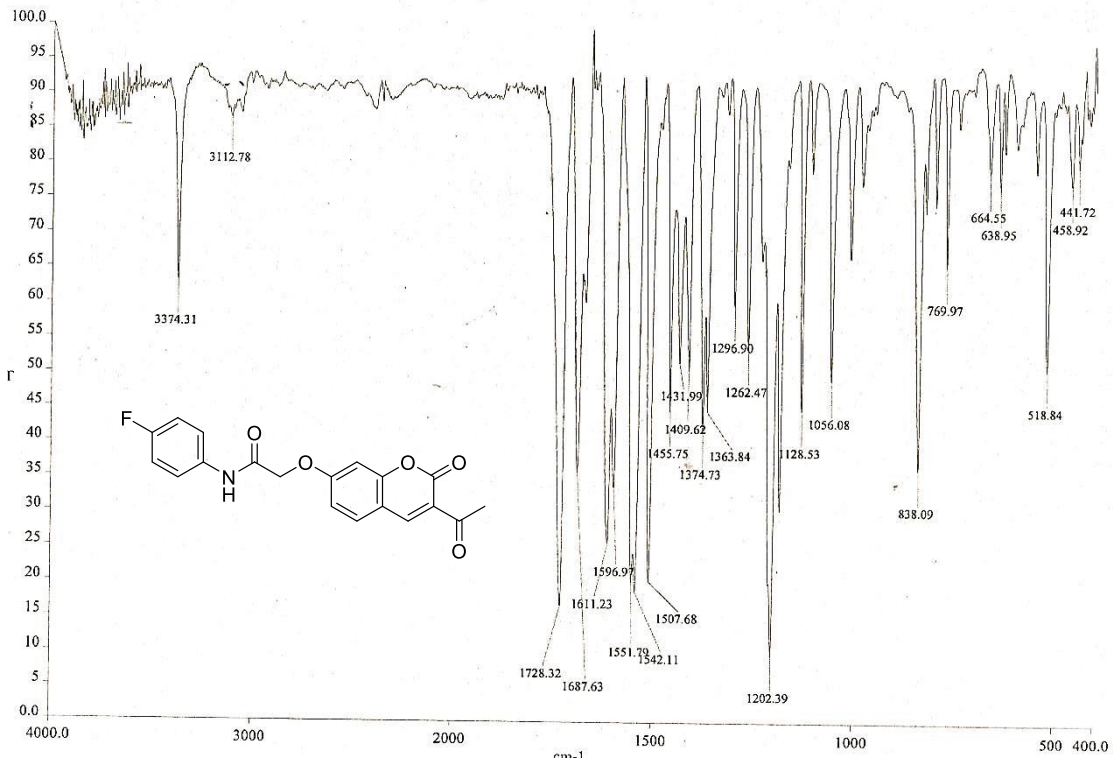

Figure-2.6.2 ^{1}H-NMR spectrum of 2-[(3-acetyl-2-oxo-2H-chromen-7-yl)oxy]-N-(4-fluorophenyl)acetamide (**8b**) in DMSO-d_6

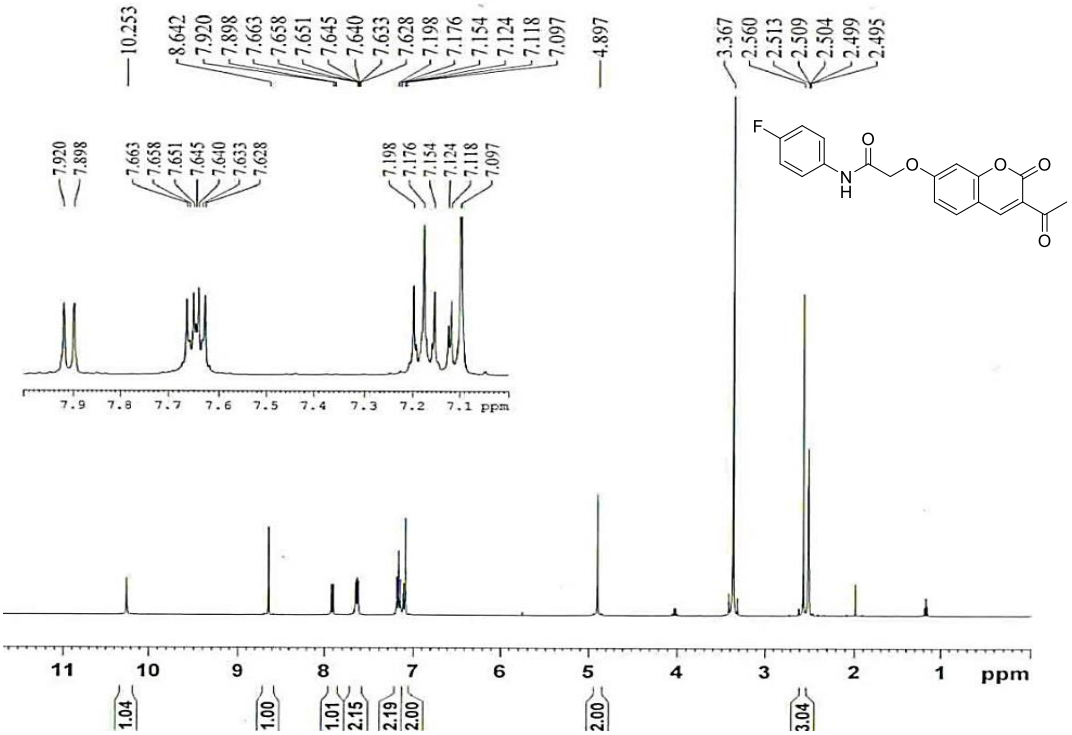

Figure-2.6.3 ^{13}C-NMR spectrum of 2-[(3-acetyl-2-oxo-2H-chromen-7-yl)oxy]-N-(4-fluorophenyl)acetamide (**8b**) in DMSO-d_6

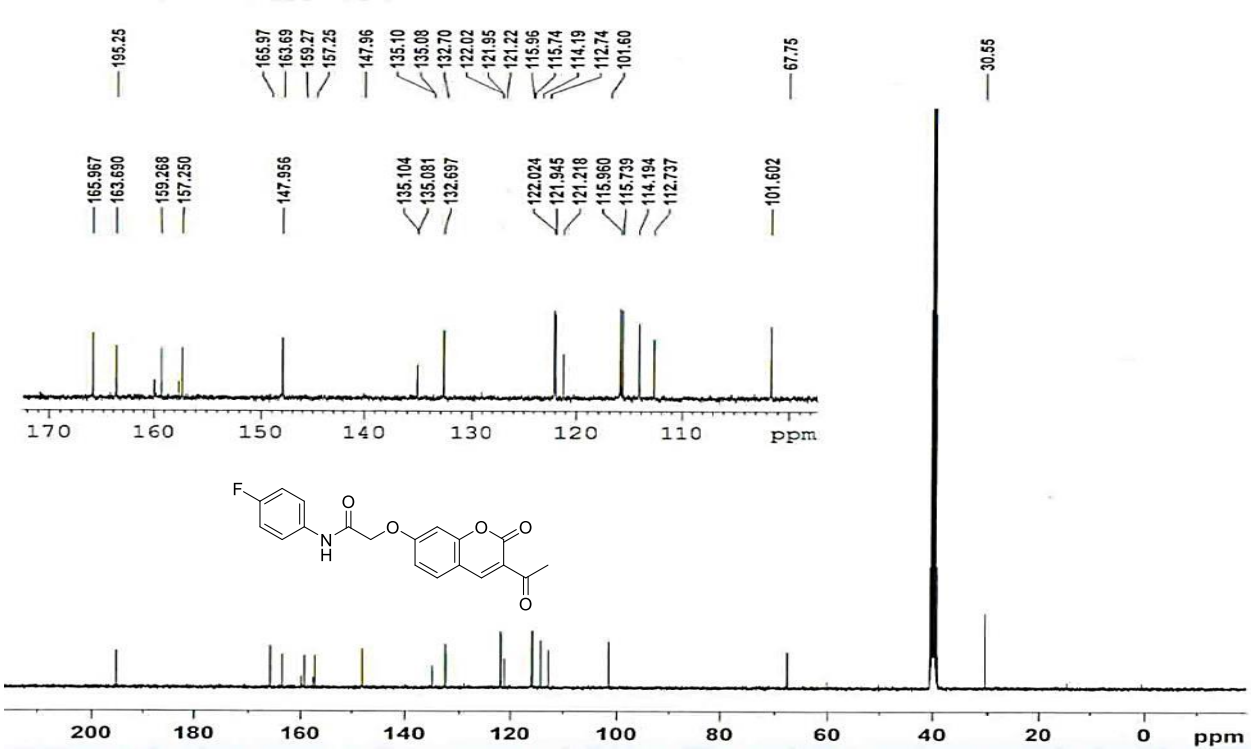

Figure-2.6.4 ESI-MS spectrum of 2-[(3-acetyl-2-oxo-2H-chromen-7-yl)oxy]-N-(4-fluorophenyl)acetamide (**8b**) M+H peak at 356.05

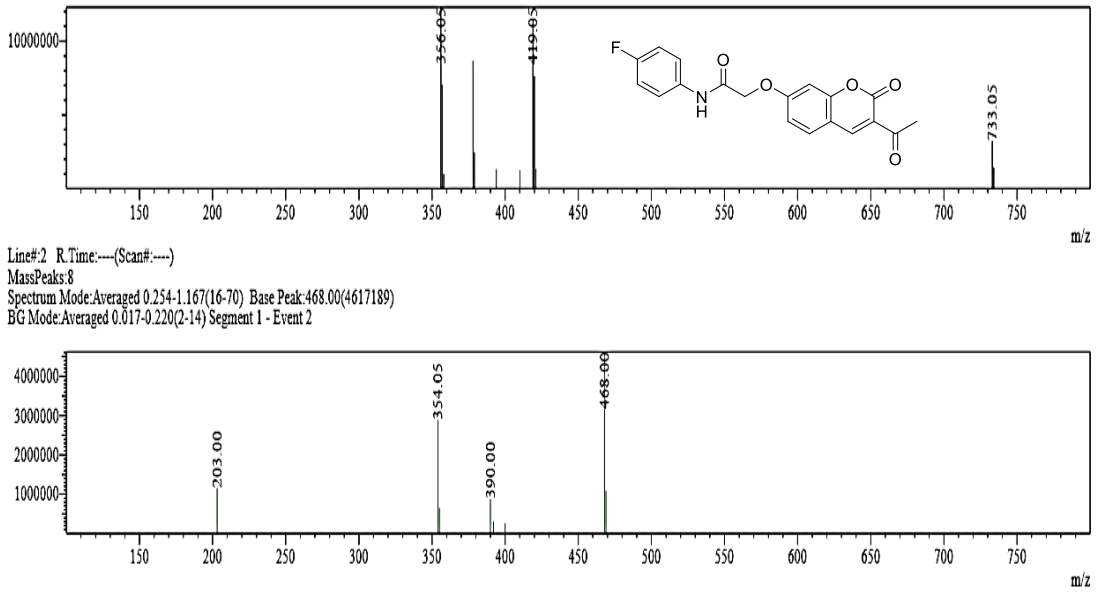

Figure-2.7.1 IR spectrum of 2-[(3-acetyl-2-oxo-2H-chromen-7-yl)oxy]-N-(4-chlorophenyl)acetamide (**8c**)

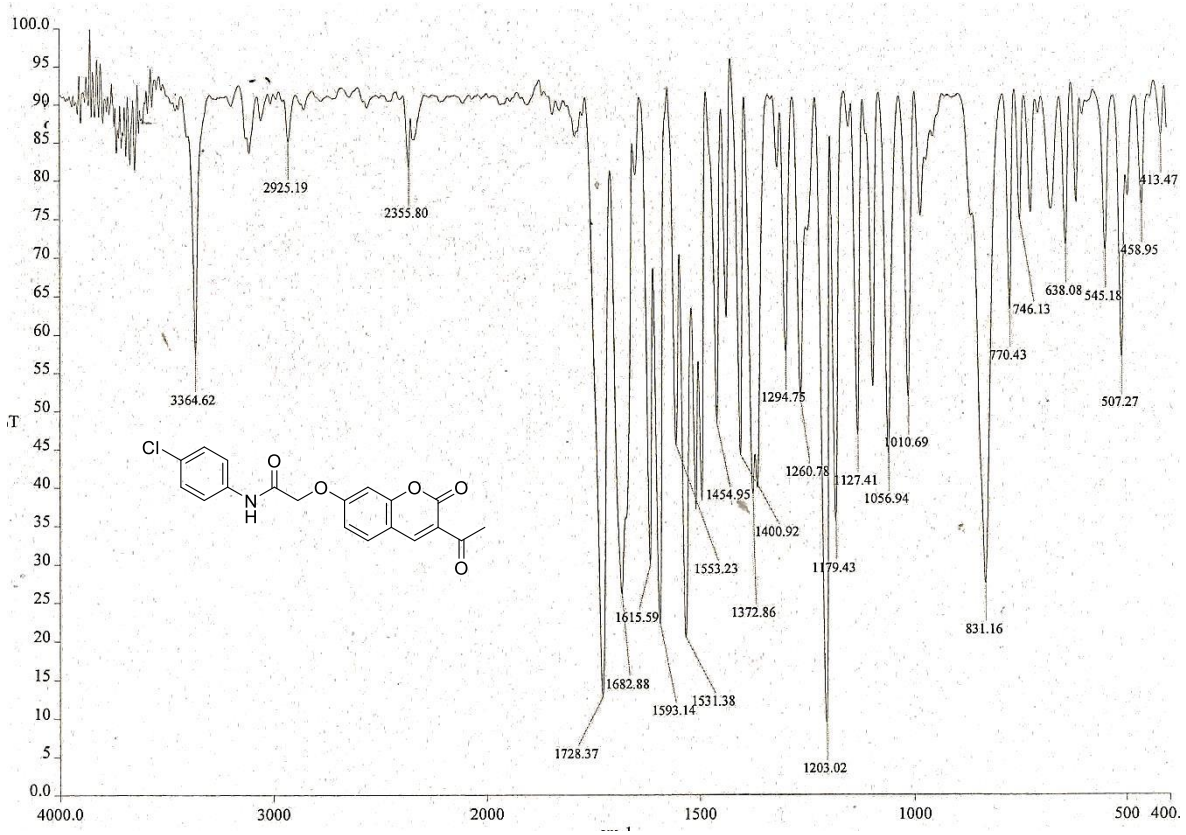

Figure-2.7.2 ^{1}H-NMR spectrum of 2-[(3-acetyl-2-oxo-2H-chromen-7-yl)oxy]-N-(4-chlorophenyl)acetamide (**8c**) in DMSO-d_6

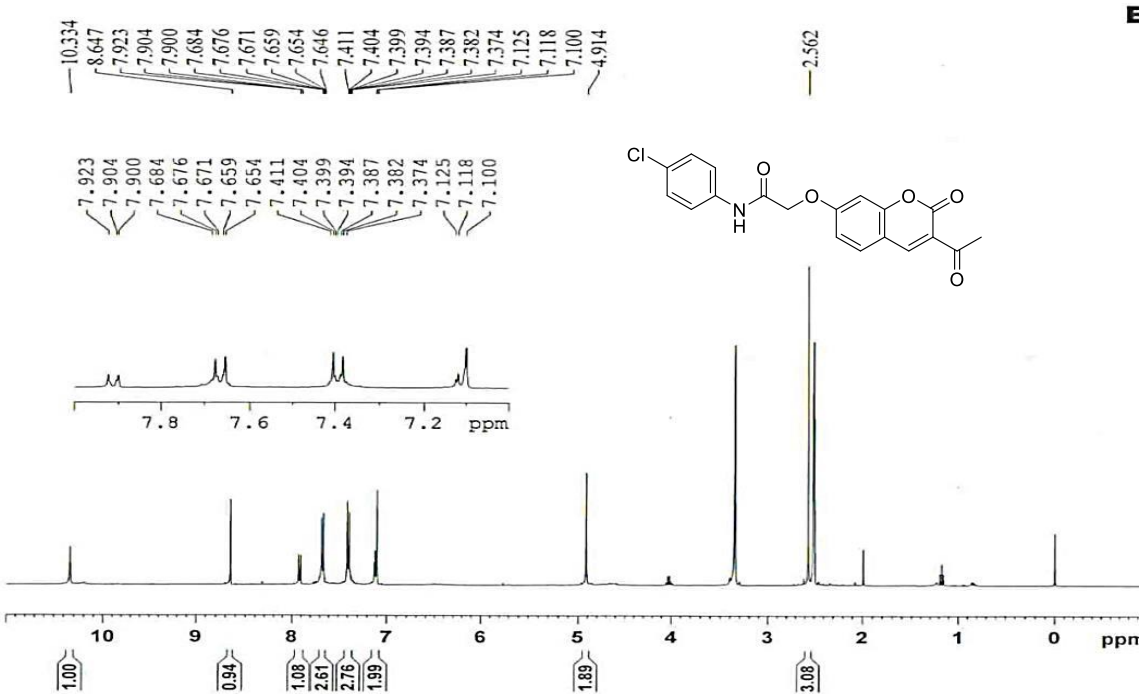

Figure-2.7.3 ^{13}C-NMR spectrum of 2-[(3-acetyl-2-oxo-2H-chromen-7-yl)oxy]-N-(4-chlorophenyl)acetamide (**8c**) in DMSO-d_6

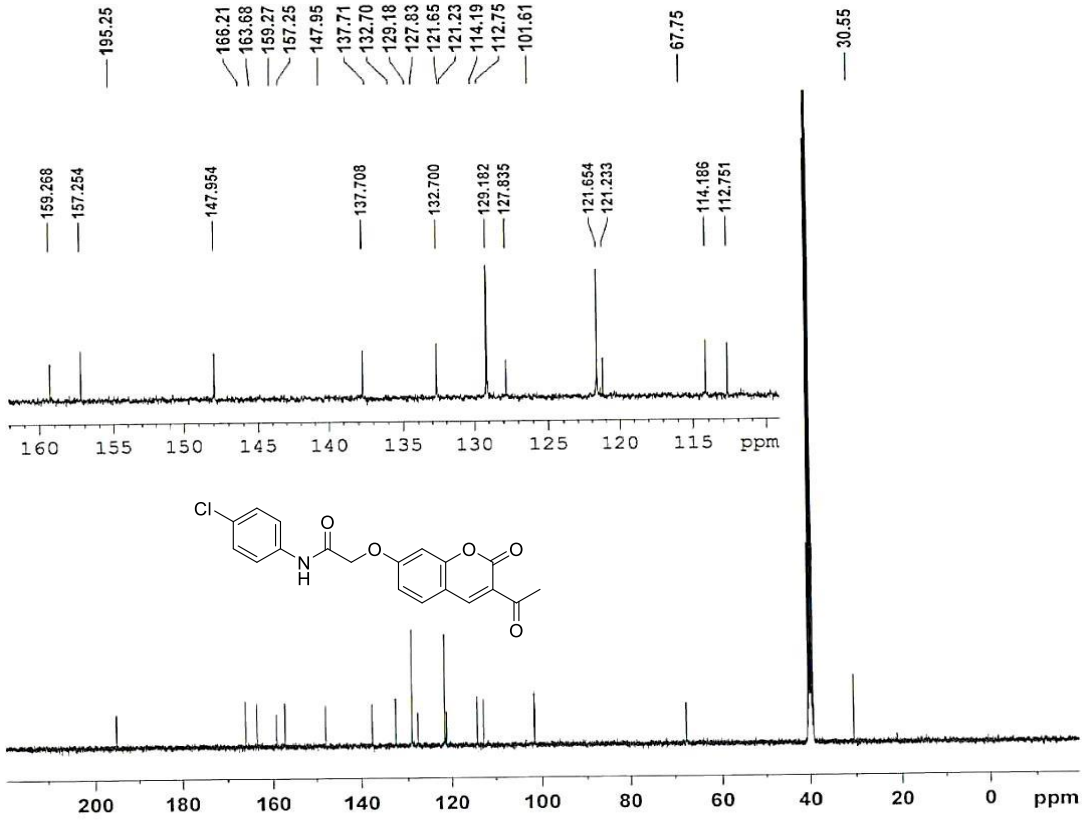

Figure-2.7.4 ESI-MS spectrum of 2-[(3-acetyl-2-oxo-2H-chromen-7-yl)oxy]-N-(4-chlorophenyl)acetamide (**8c**) M-H peak at 370.00

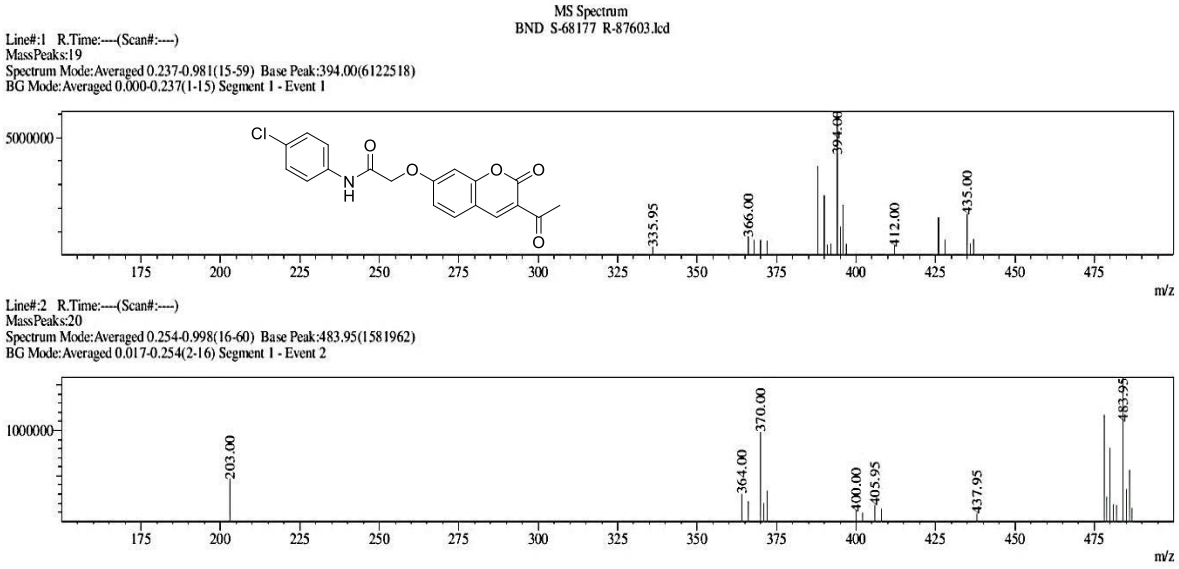

Figure-2.8.1 IR spectrum of 2-[(3-acetyl-2-oxo-2H-chromen-7-yl)oxy]-N-(3-fluorophenyl)acetamide (**8d**)

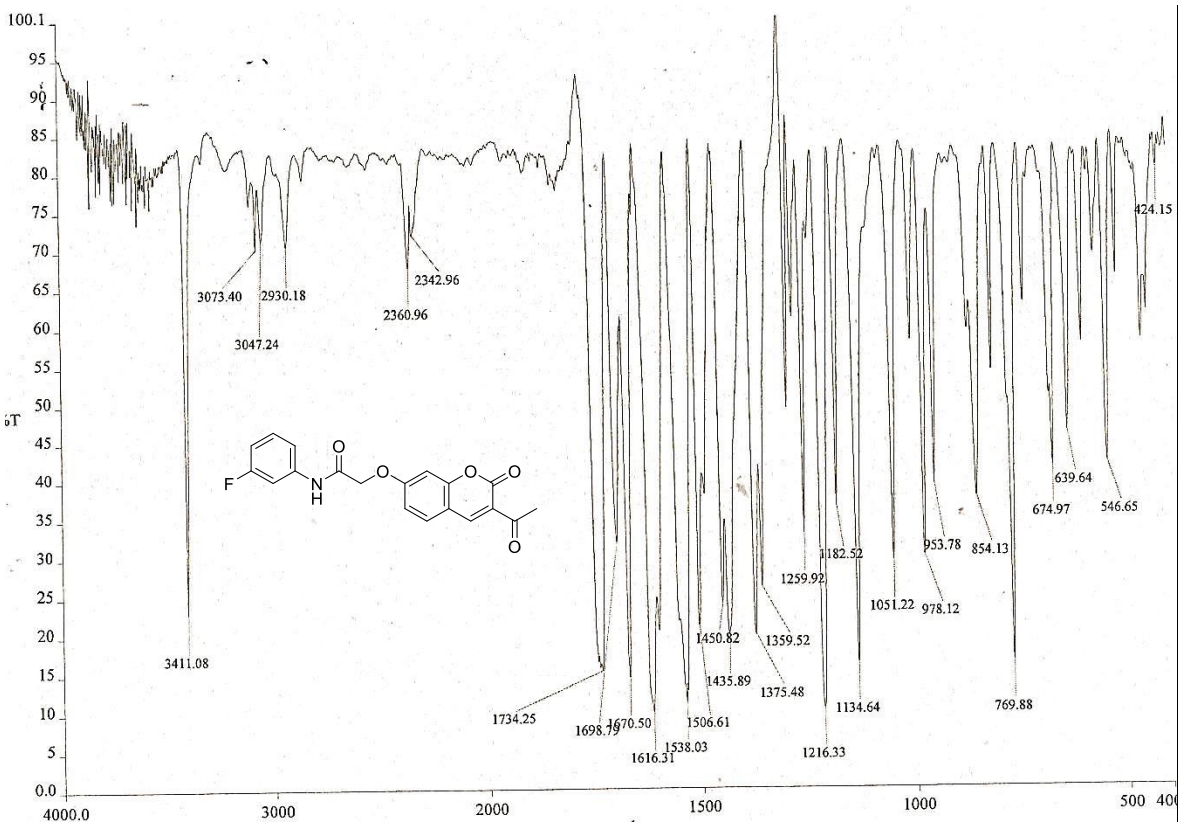

Figure-2.8.2 ^{1}H-NMR spectrum of 2-[(3-acetyl-2-oxo-2H-chromen-7-yl)oxy]-N-(3-fluorophenyl)acetamide (**8d**) in DMSO-d_6

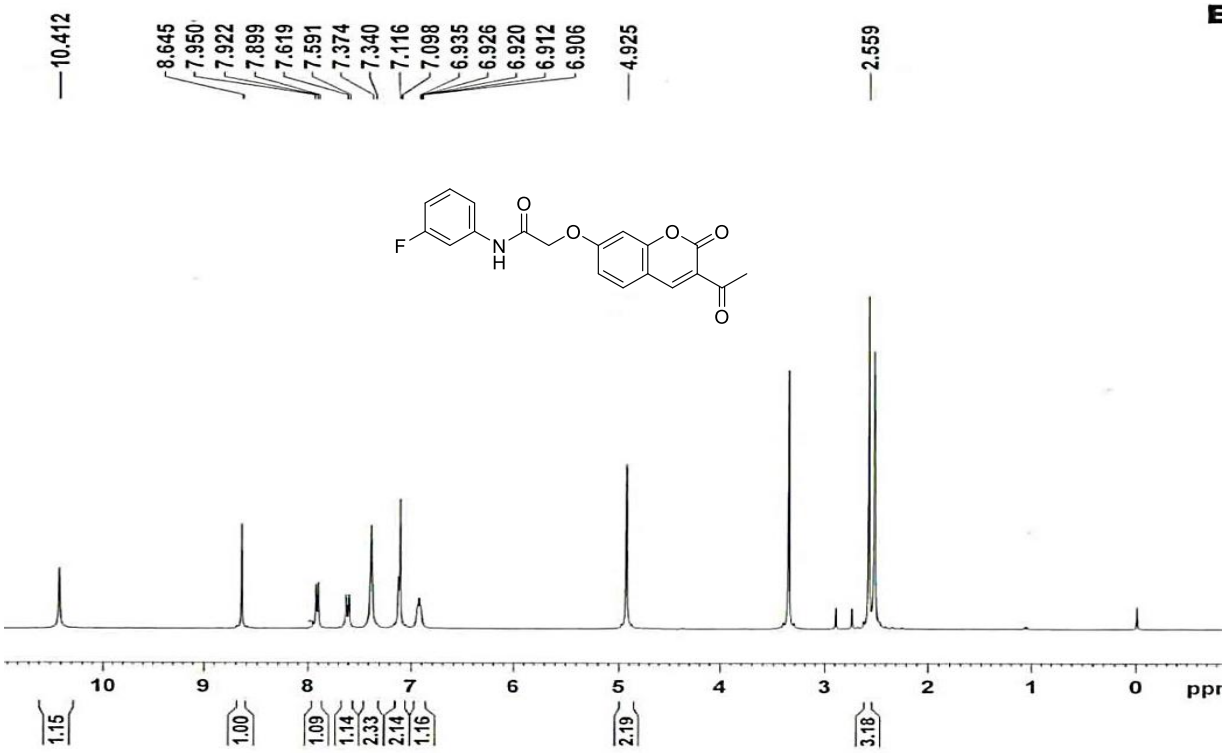

Figure-2.8.3 ^{13}C-NMR spectrum of 2-[(3-acetyl-2-oxo-2H-chromen-7-yl)oxy]-N-(3-fluorophenyl)acetamide (**8d**)

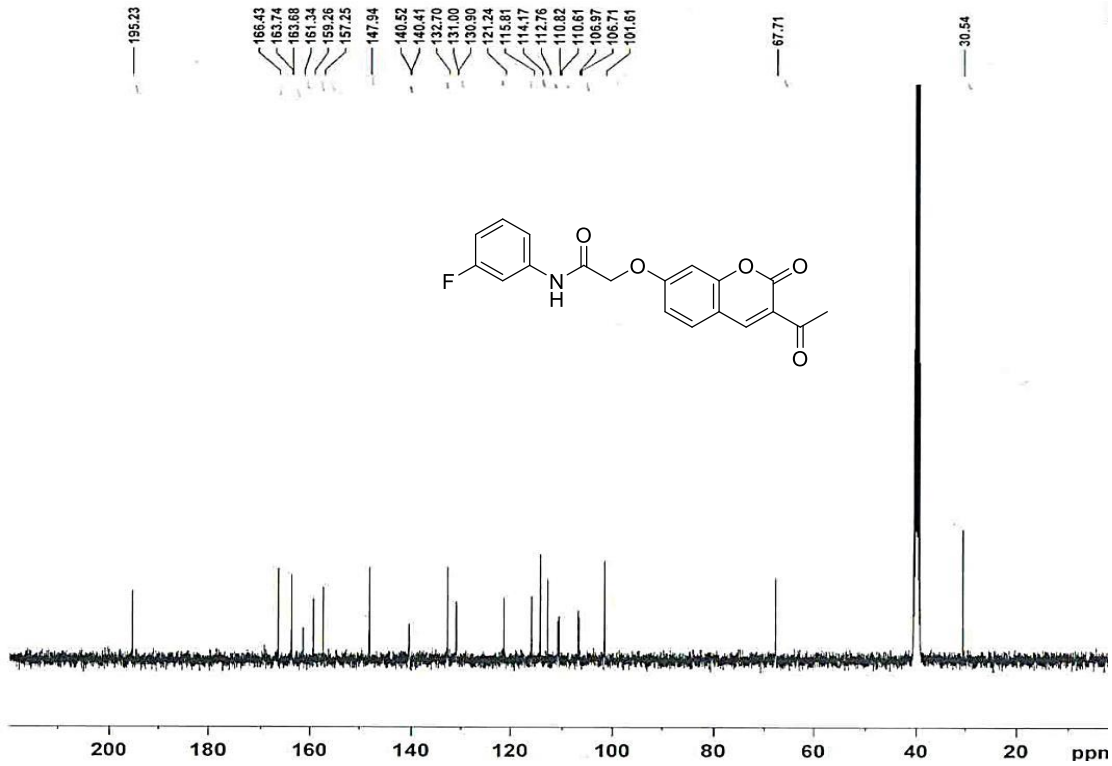

Figure-2.9.1 IR spectrum of 2-[(3-acetyl-2-oxo-2H-chromen-7-yl)oxy]-N-(3-chlorophenyl)acetamide (**8e**)

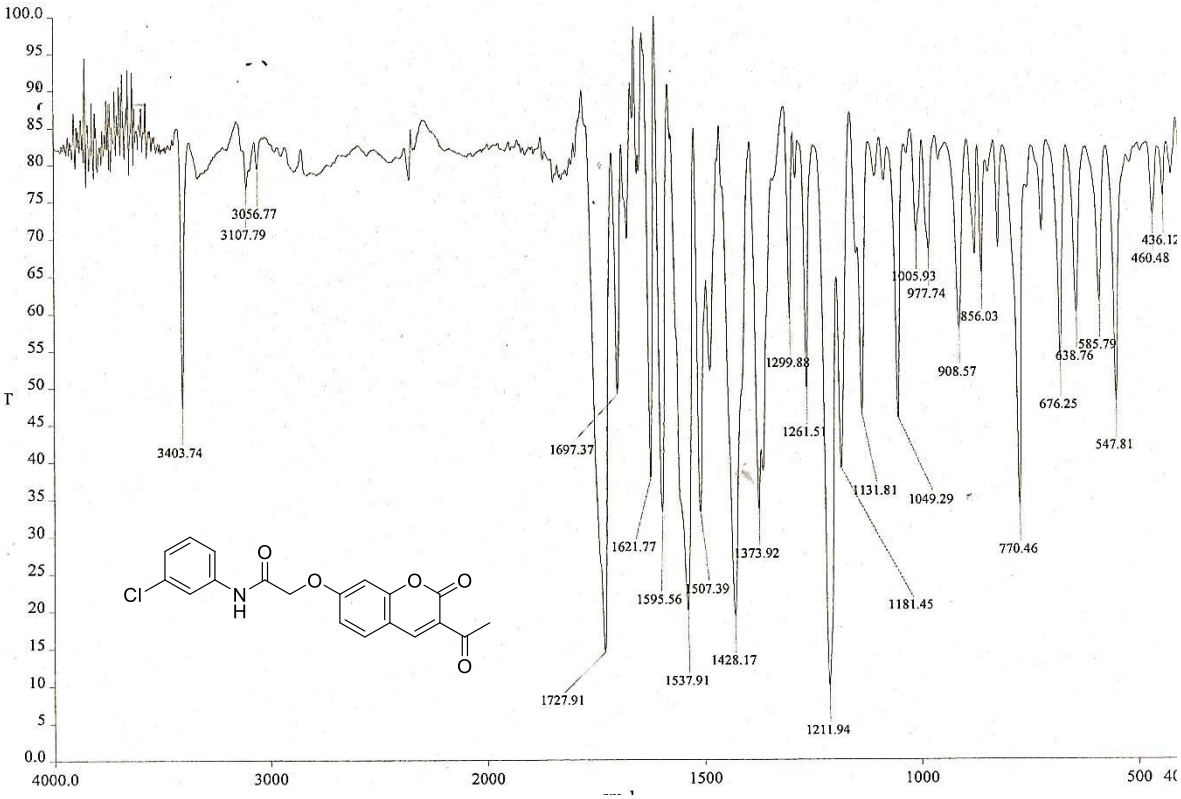

Figure-2.9.2 ^{1}H-NMR spectrum of 2-[(3-acetyl-2-oxo-2H-chromen-7-yl)oxy]-N-(3-chlorophenyl)acetamide (**8e**) in DMSO-d_6

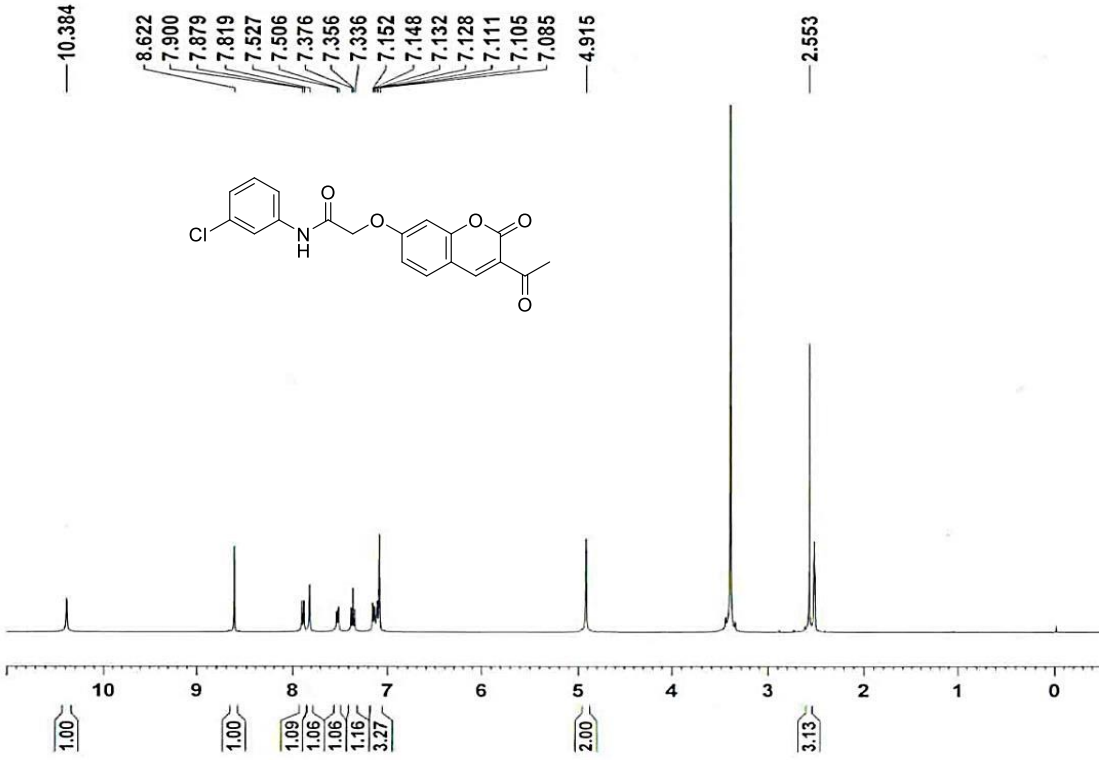

Figure-2.9.3 D_2O exchange ^{1}H-NMR spectrum of 2-[(3-acetyl-2-oxo-2H-chromen-7-yl)oxy]-N-(3-chlorophenyl)acetamide (**8e**) in DMSO-d_6

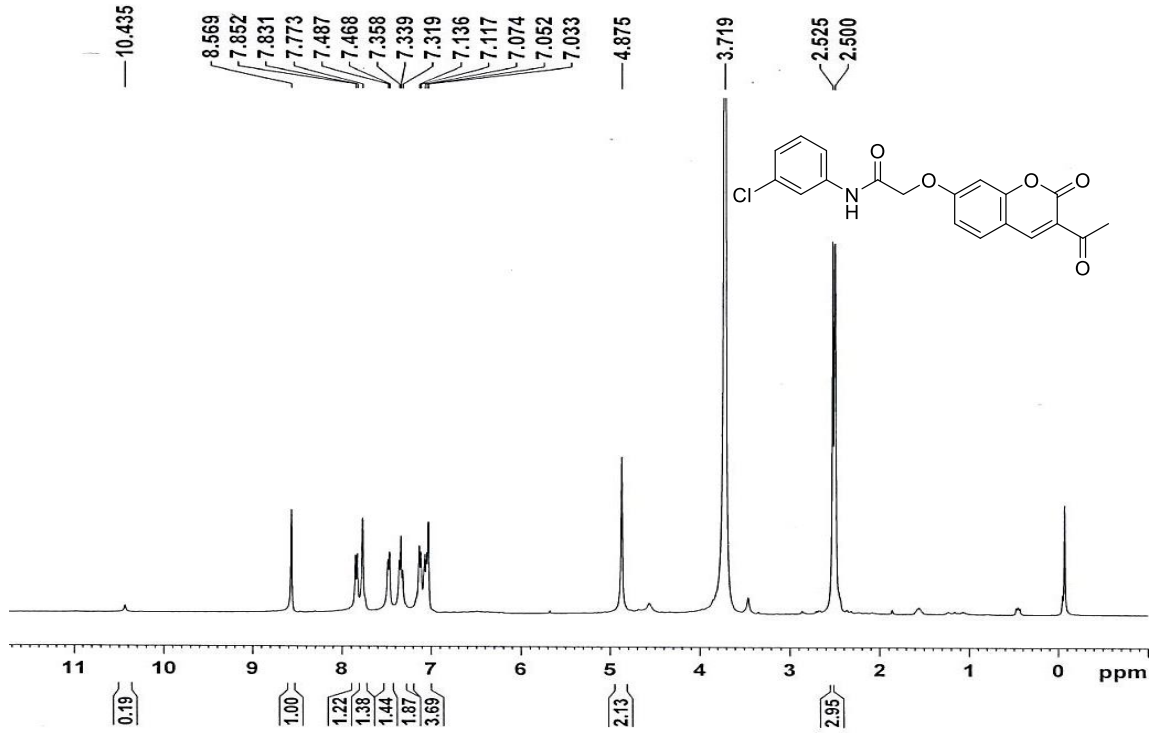

Figure-2.9.4 ^{13}C-NMR spectrum of 2-[(3-acetyl-2-oxo-2H-chromen-7-yl)oxy]-N-(3-chlorophenyl)acetamide (**8e**) in DMSO-d_6

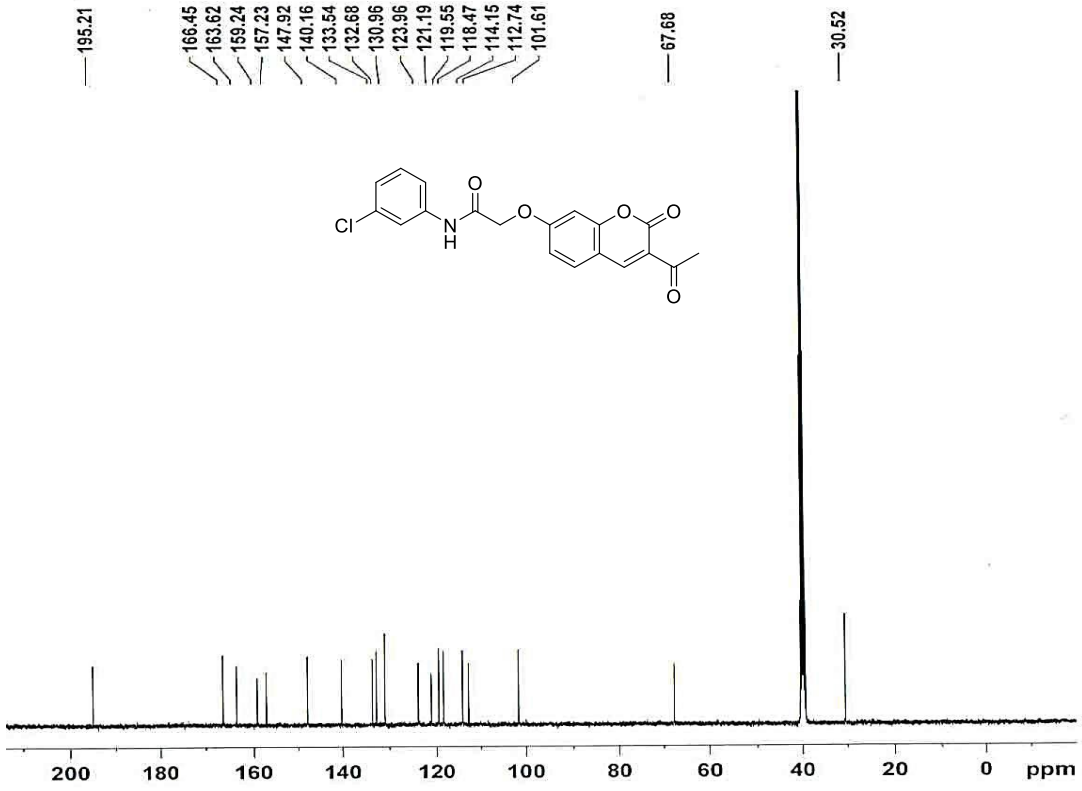

Figure-2.9.5 ESI-MS spectrum of 2-[(3-acetyl-2-oxo-2H-chromen-7-yl)oxy]-N-(3-chlorophenyl)acetamide (**8e**) M-H peak at 370.00

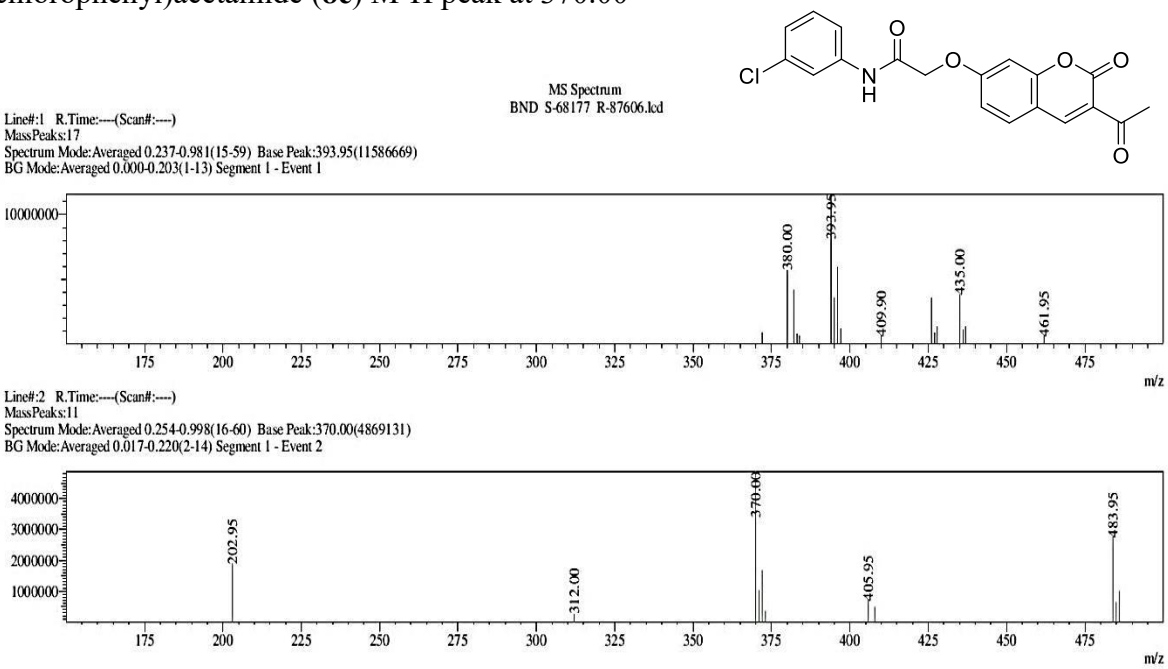

Figure-2.10.1 IR spectrum of 3-acetyl-7-[2-oxo-2-(pyrrolidin-1-yl)ethoxy]-2H-chromen-2-one (**8f**)

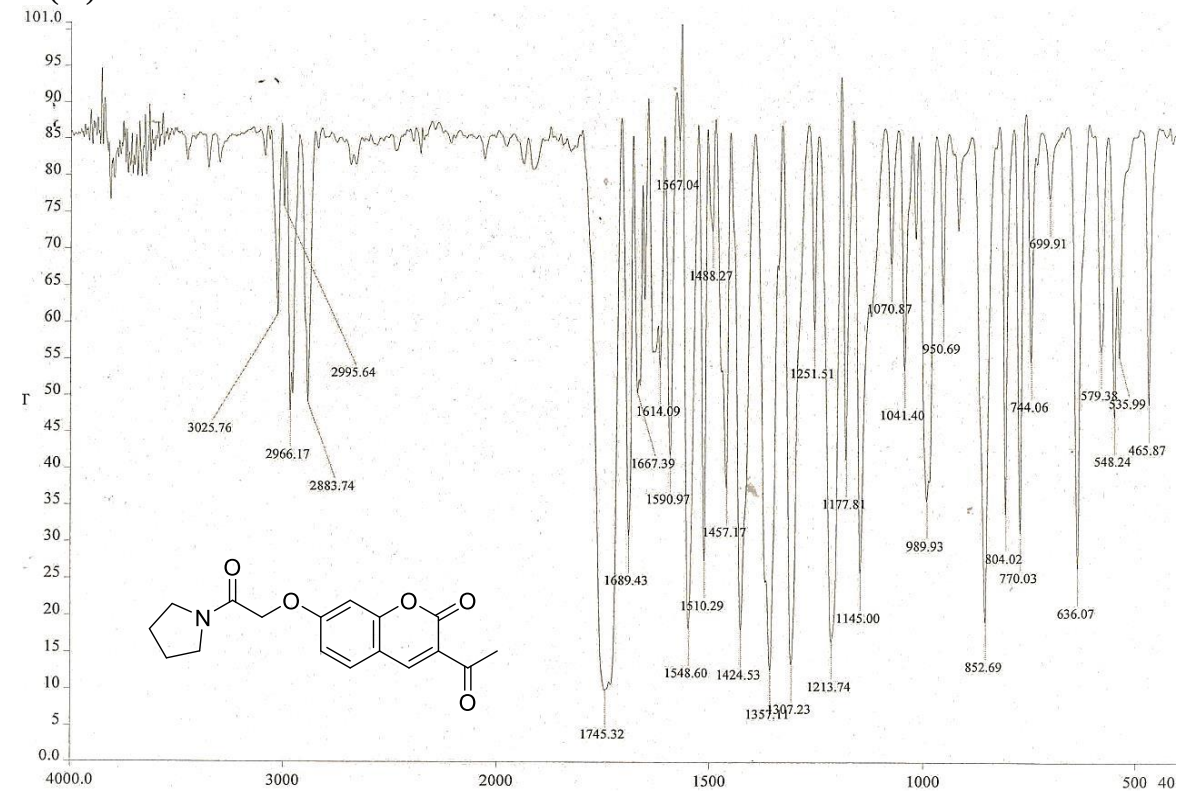

Figure-2.10.2 ^{1}H-NMR spectrum of 3-acetyl-7-[2-oxo-2-(pyrrolidin-1-yl)ethoxy]-2H-chromen-2-one (**8f**) in $CDCl_3$

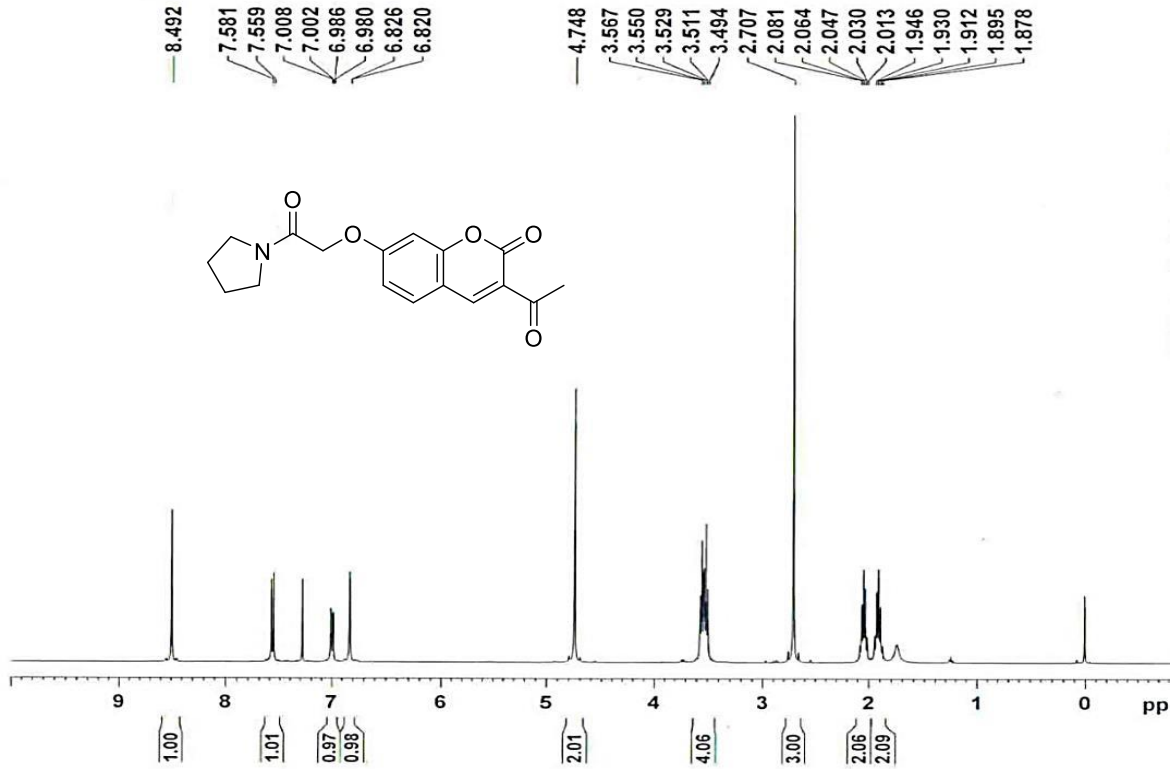

Figure-2.10.3 ^{13}C-NMR spectrum of 3-acetyl-7-[2-oxo-2-(pyrrolidin-1-yl)ethoxy]-2H-chromen-2-one (**8f**) in CDC_{l3}

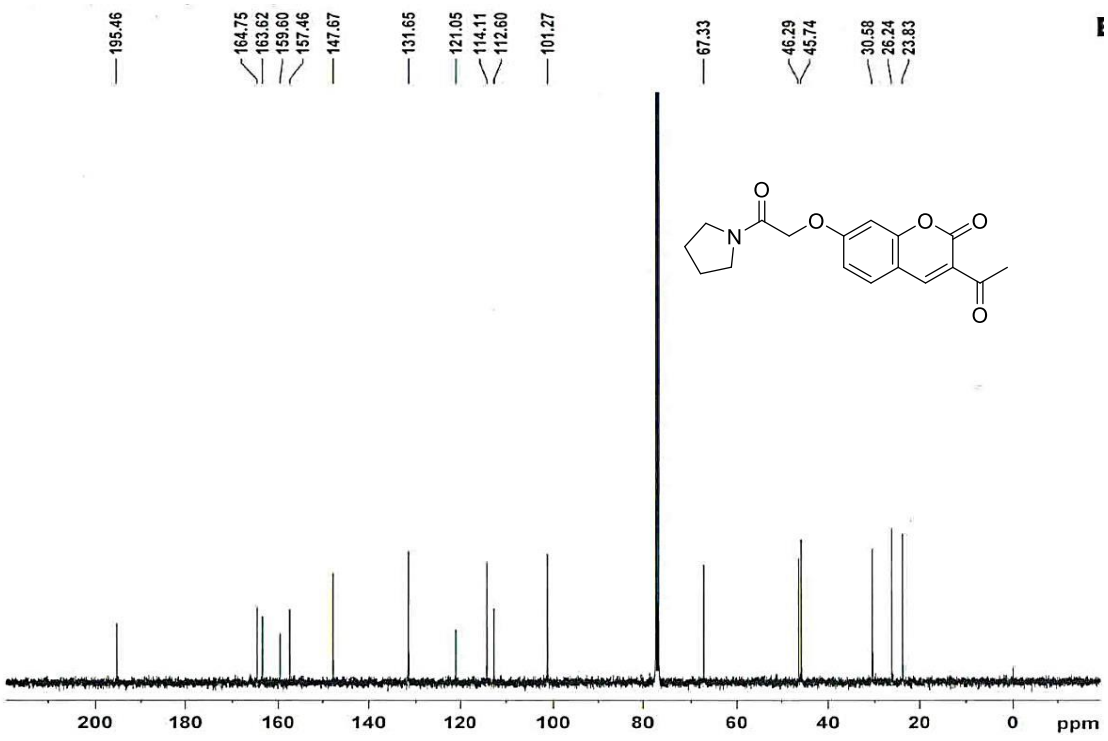

Figure-2.10.4 ESI-MS spectrum of 3-acetyl-7-[2-oxo-2-(pyrrolidin-1-yl)ethoxy]-2H-chromen-2-one (**8f**) M+H peak at 316.95

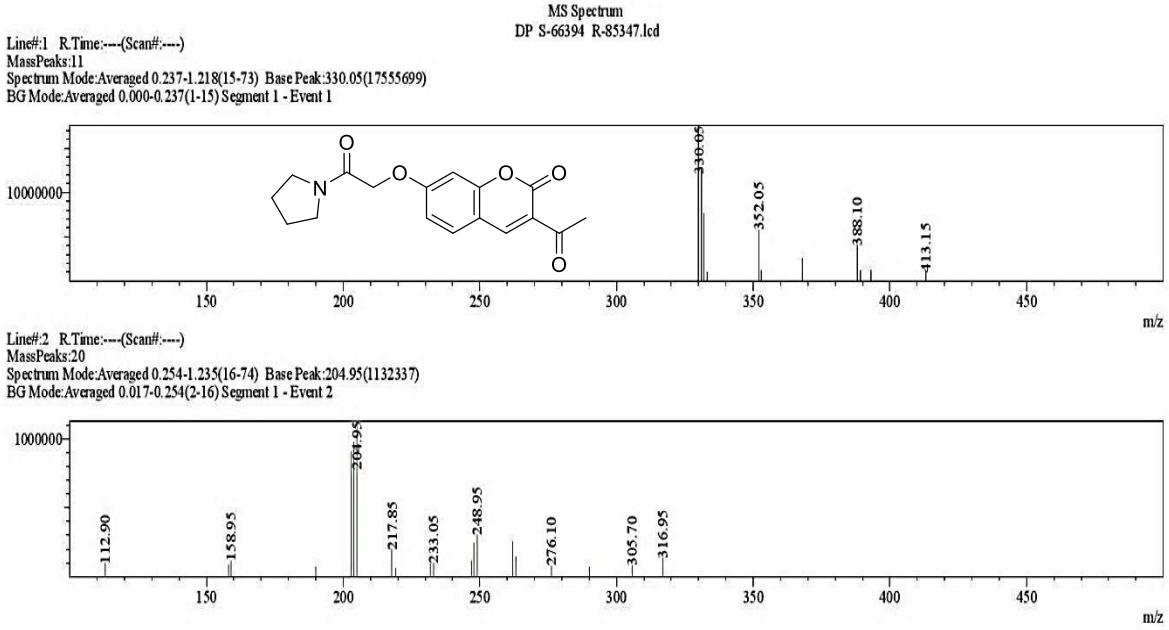

Figure-2.11.1 IR spectrum of 3-acetyl-7-[2-oxo-2-(piperidin-1-yl)ethoxy]-2H-chromen-2-one (**8g**)

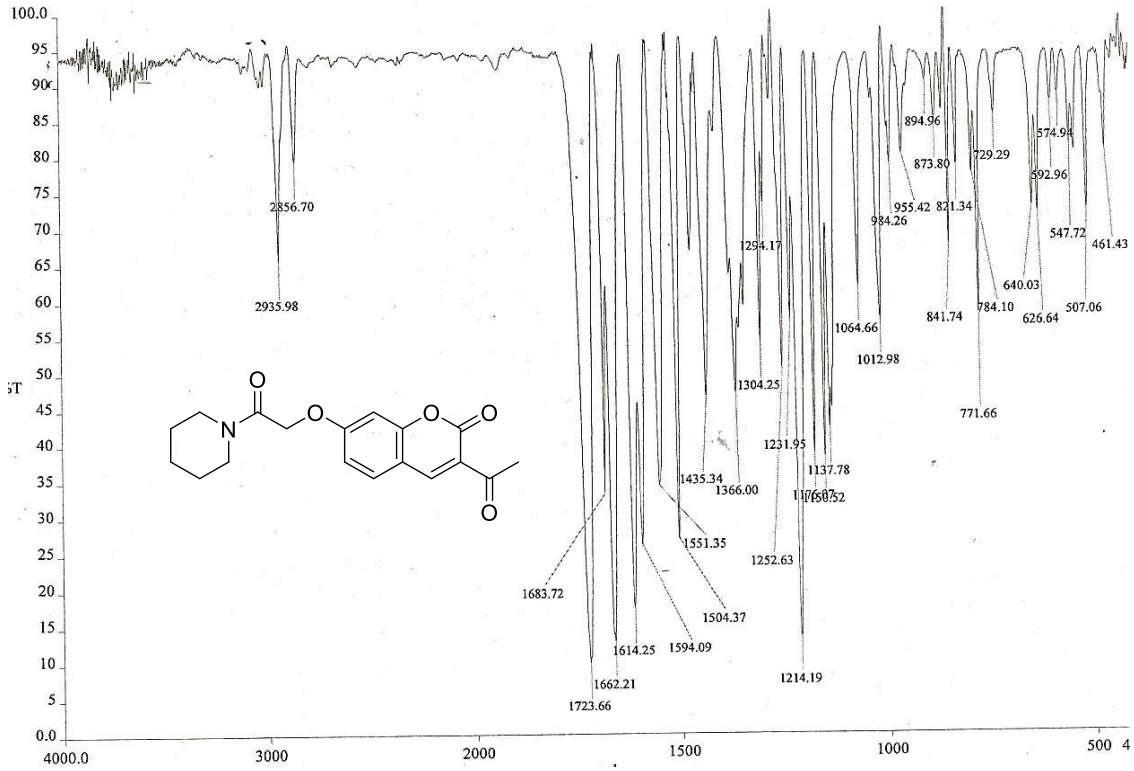

Figure-2.11.2 ^{1}H-NMR spectrum of 3-acetyl-7-[2-oxo-2-(piperidin-1-yl)ethoxy]-2H-chromen-2-one (**8g**) in $CDCl_3$

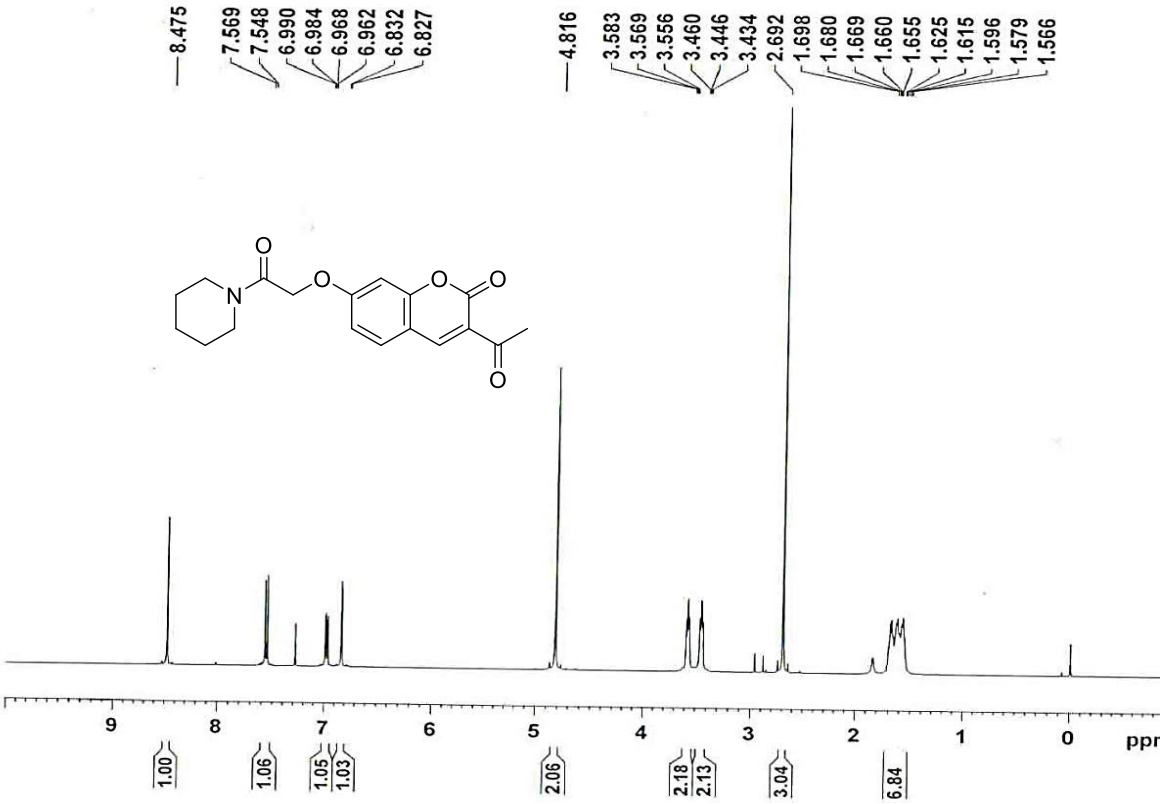

Figure-2.11.3 ^{13}C-NMR spectrum of 3-acetyl-7-[2-oxo-2-(piperidin-1-yl)ethoxy]-2H-chromen-2-one (**8g**) in $CDCl_3$

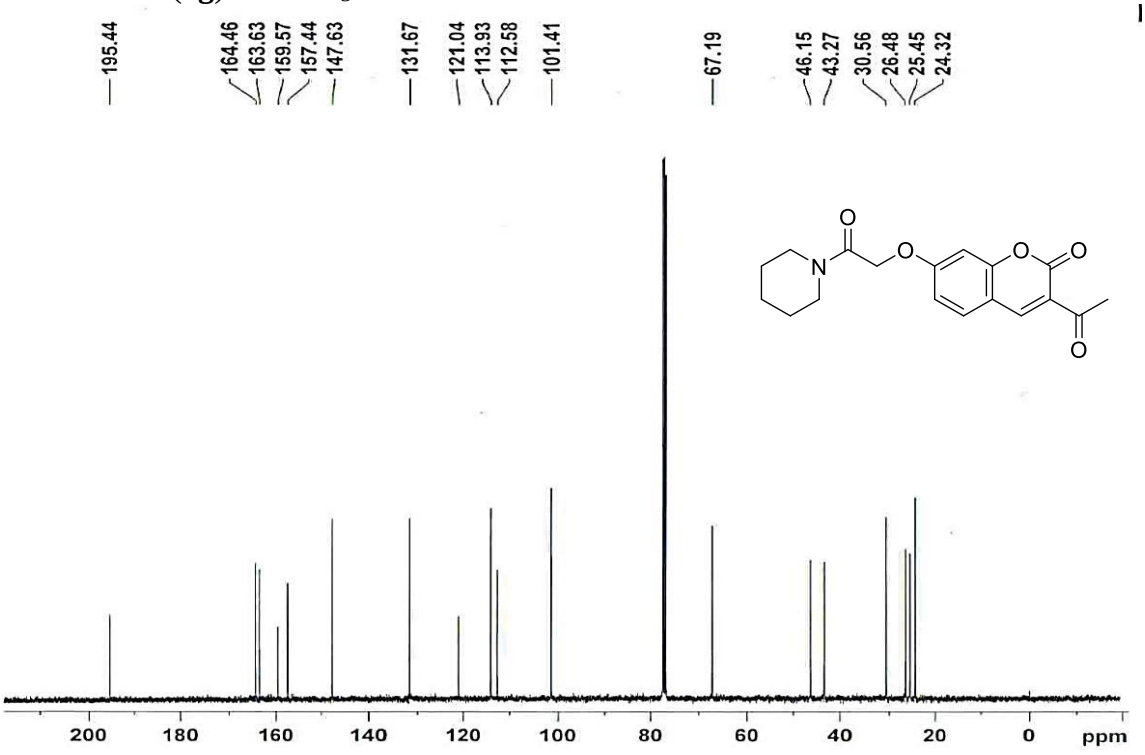

Figure-2.11.4 ESI-MS spectrum of 3-acetyl-7-[2-oxo-2-(piperidin-1-yl)ethoxy]-2H-chromen-2-one (**8g**) M+H peak at 330.05

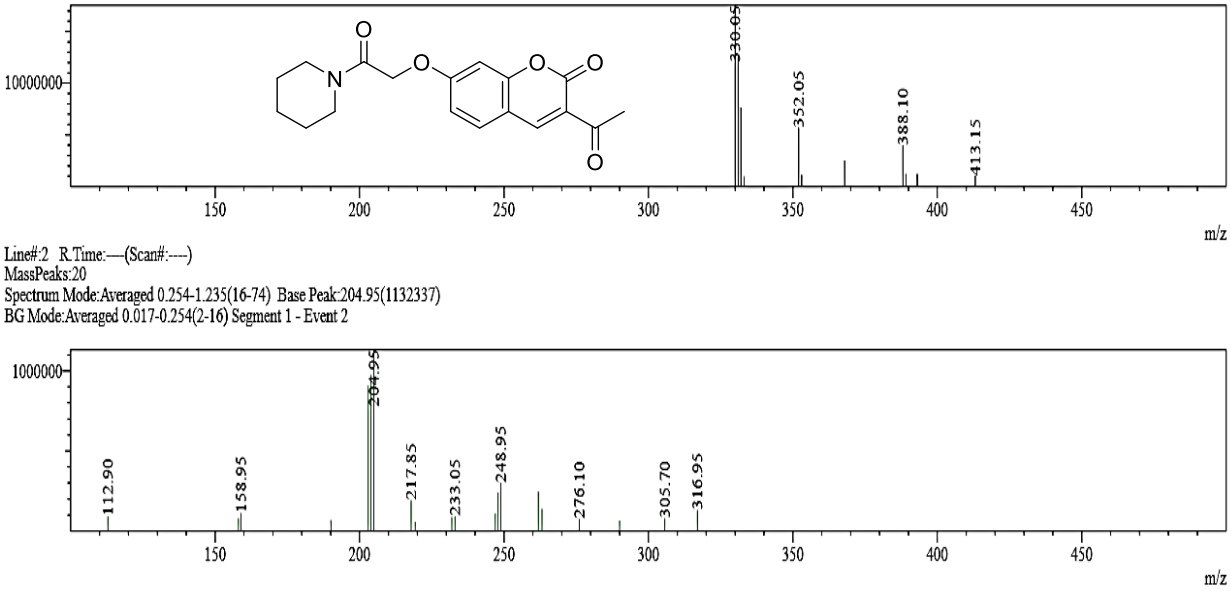

Figure-2.12.1 IR spectrum of ethyl 7-{2-[(4-methylphenyl)amino]-2-oxoethoxy}-2-oxo-2H-chromene-3-carboxylate (**10a**)

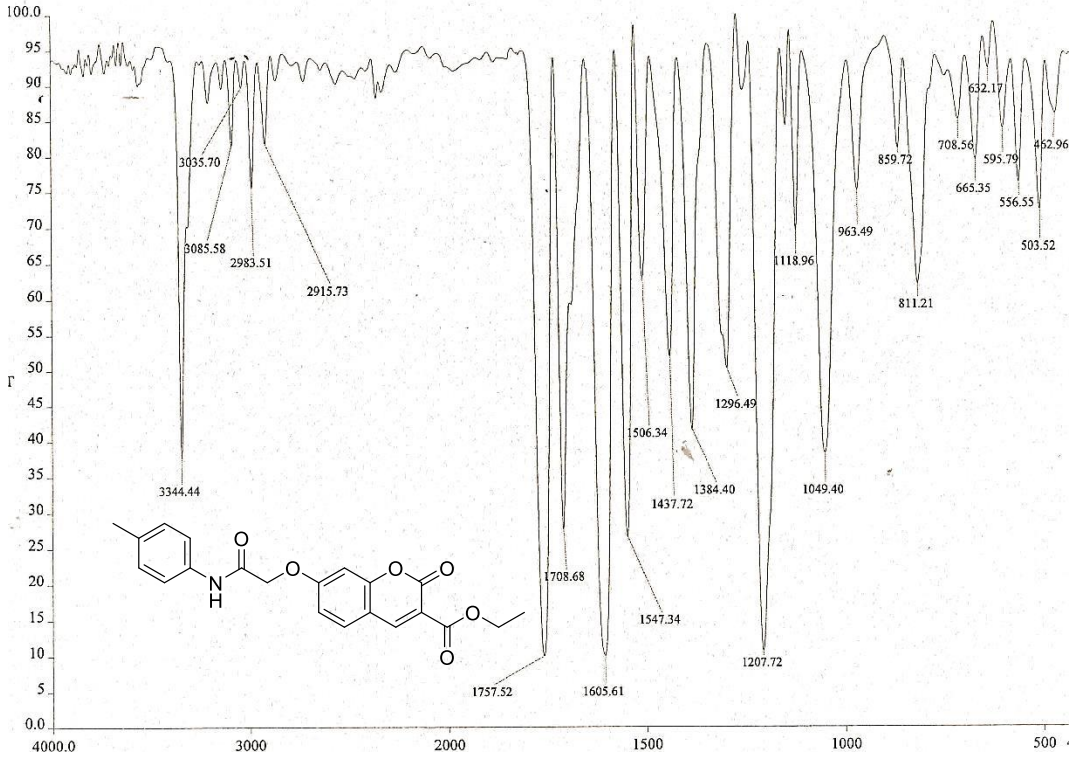

Figure-2.12.2 ^{1}H-NMR spectrum of ethyl 7-{2-[(4-methylphenyl)amino]-2-oxoethoxy}-2-oxo-2H-chromene-3-carboxylate (**10a**) in CDCl3

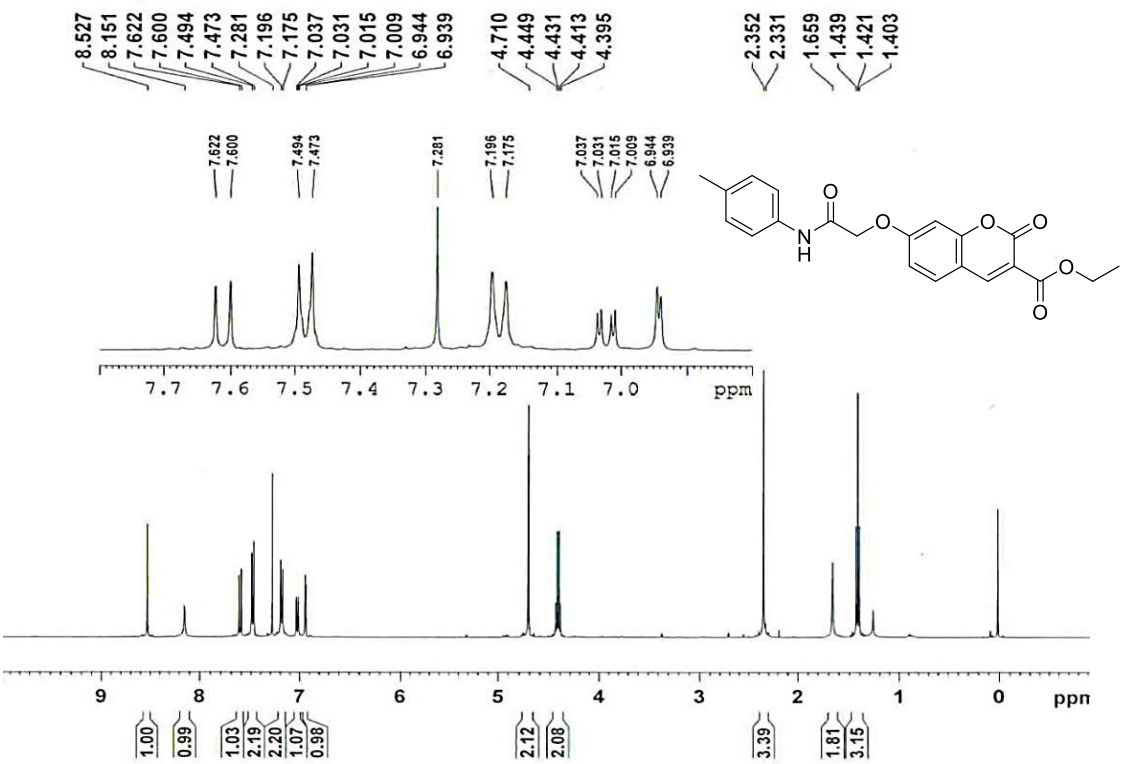

Figure-2.12.3 D_2O exchange ^{1}H-NMR spectrum of ethyl 7-{2-[(4-methylphenyl)amino]-2-oxoethoxy}-2-oxo-2H-chromene-3-carboxylate (**10a**) in $CDCl_3$

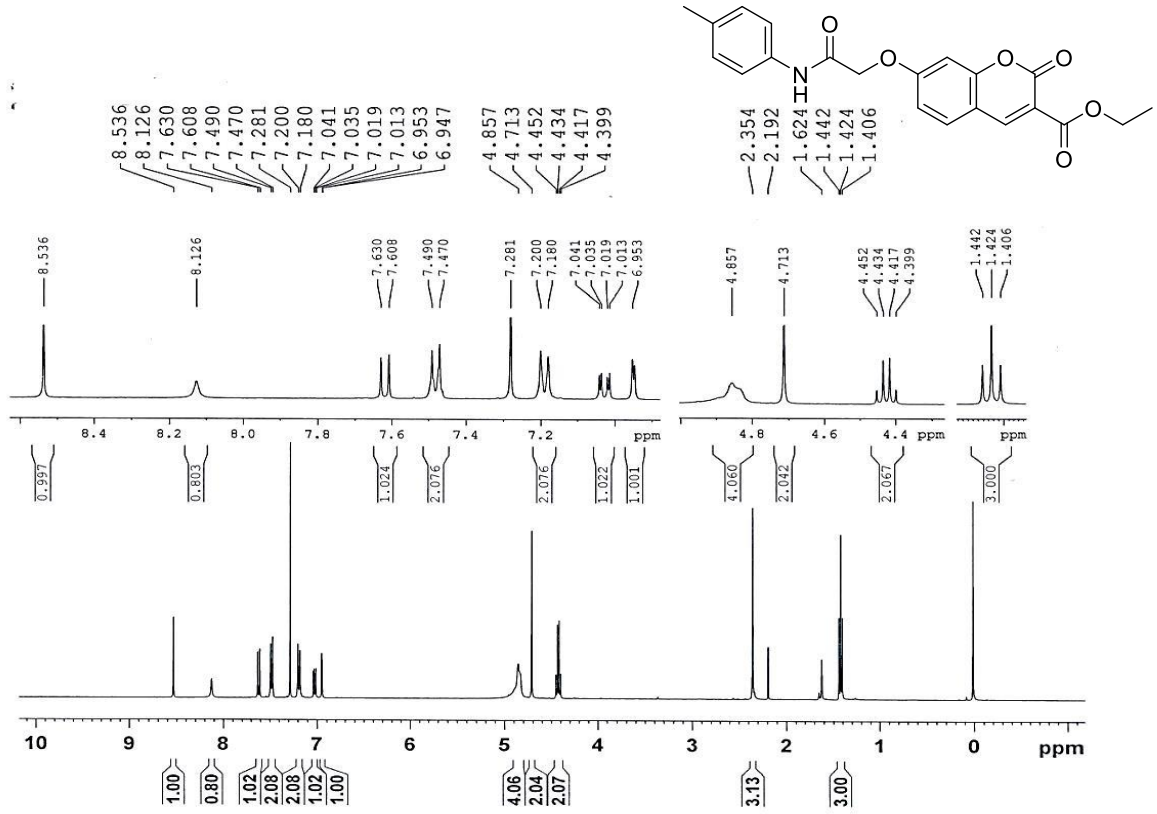

Figure-2.12.4 ^{13}C-NMR spectrum of ethyl 7-{2-[(4-methylphenyl)amino]-2-oxoethoxy}-2-oxo-2H-chromene-3-carboxylate (**10a**) in $CDCl_3$

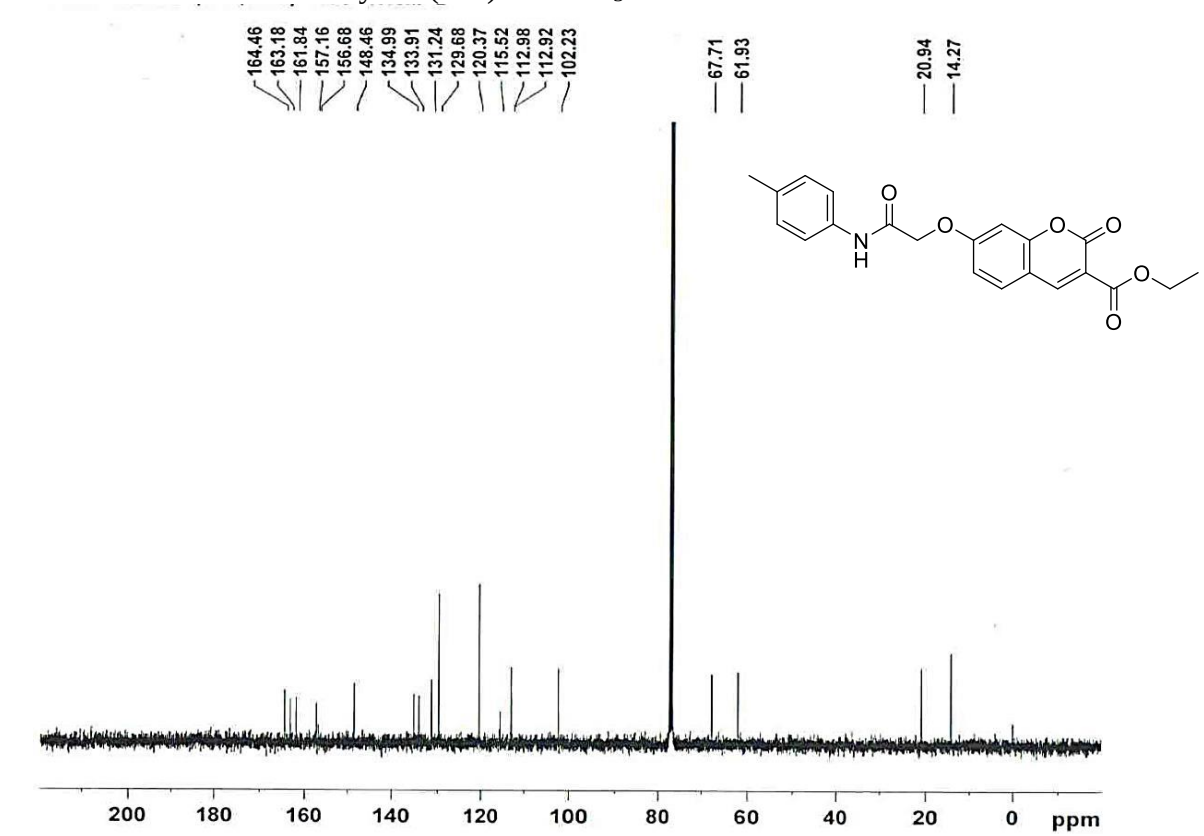

Figure-2.12.5 ESI-MS spectrum of ethyl 7-{2-[(4-methylphenyl)amino]-2-oxoethoxy}-2-oxo-2H-chromene-3-carboxylate (**10a**) M+H peak at 382.05

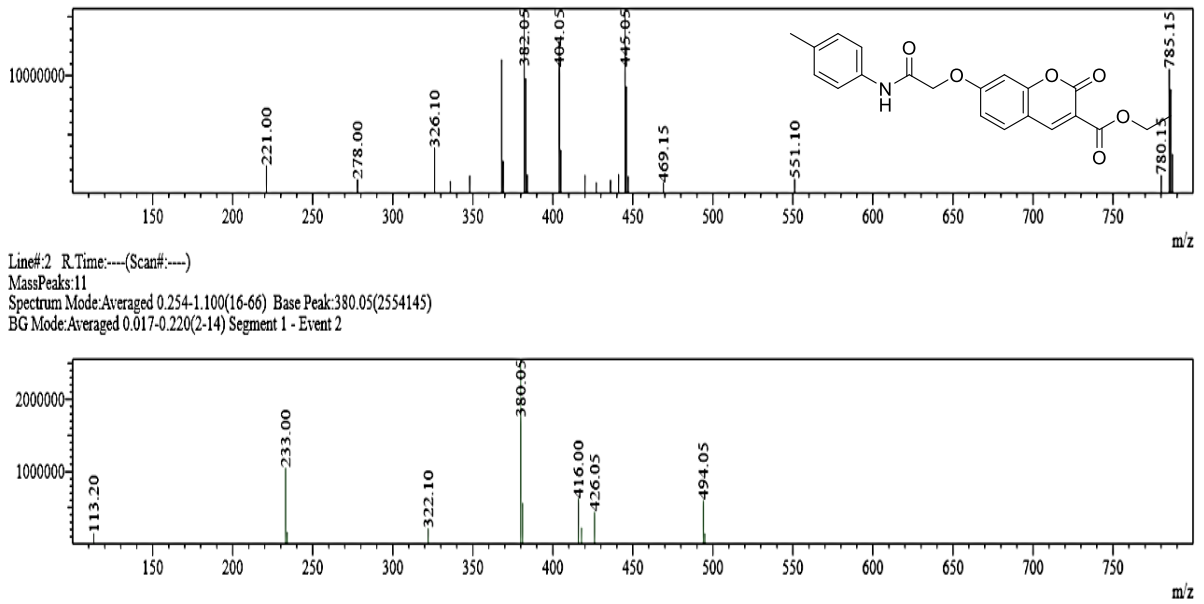

Figure-2.13.1 IR spectrum of ethyl 2-oxo-7-[2-oxo-2-(pyrrolidin-1-yl)ethoxy]-2H-chromene-3-carboxylate (**10b**)

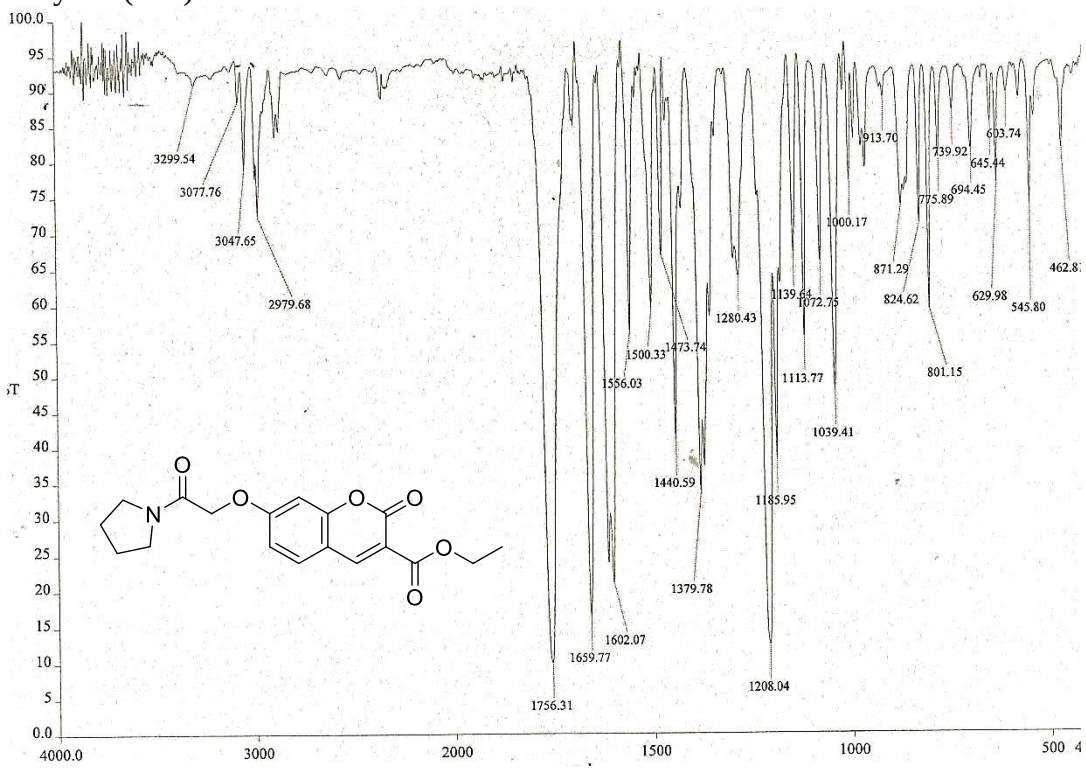

Figure-2.13.2 ^{1}H-NMR spectrum of ethyl 2-oxo-7-[2-oxo-2-(pyrrolidin-1-yl)ethoxy]-2H-chromene-3-carboxylate (**10b**) in DMSO-d_6

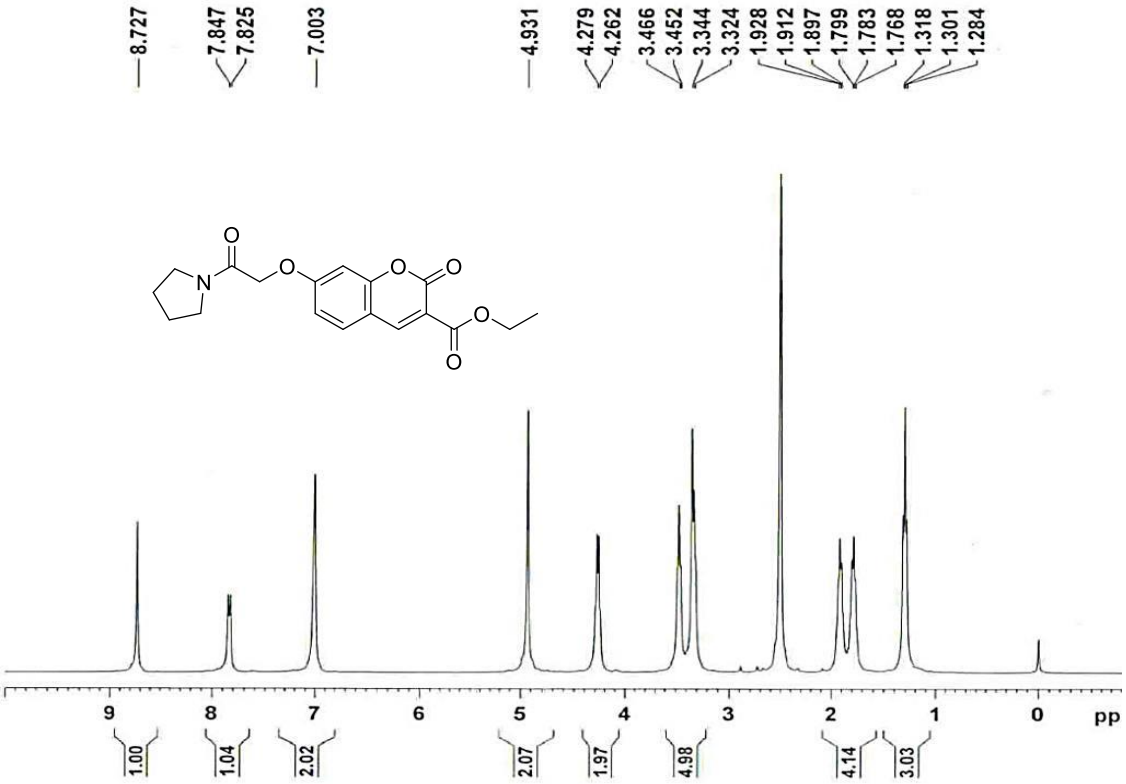

Figure-2.13.3 ^{13}C-NMR spectrum of ethyl 2-oxo-7-[2-oxo-2-(pyrrolidin-1-yl)ethoxy]-2H-chromene-3-carboxylate (**10b**) in DMSO-d_6

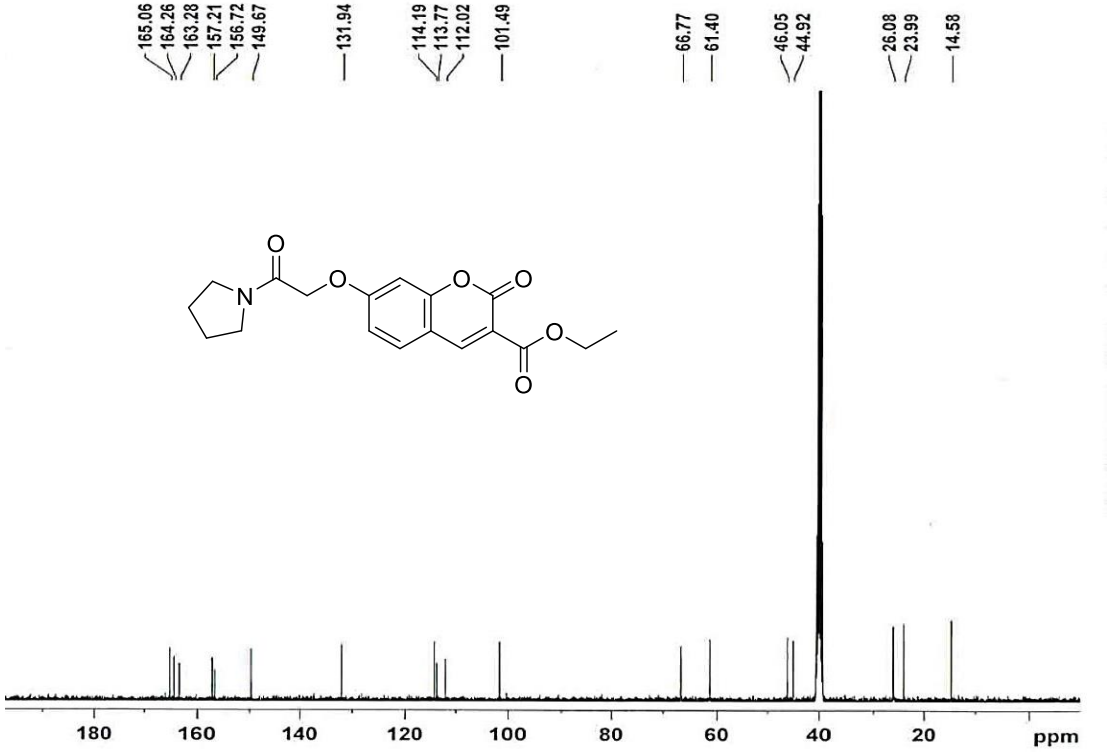

Figure-2.13.4 ESI-MS spectrum of ethyl 2-oxo-7-[2-oxo-2-(pyrrolidin-1-yl)ethoxy]-2H-chromene-3-carboxylate (**10b**) M+H peak at 346.05

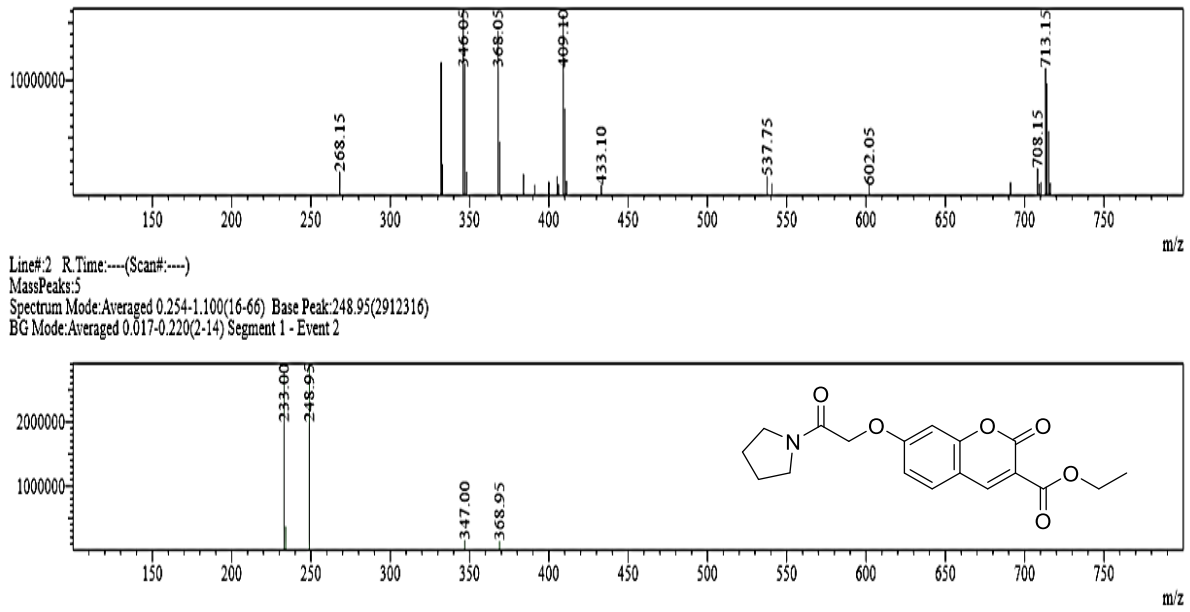

Figure-2.14.1 IR spectrum of ethyl 2-oxo-7-[2-oxo-2-(piperidin-1-yl)ethoxy]-2H-chromene-3-carboxylate (**10c**)

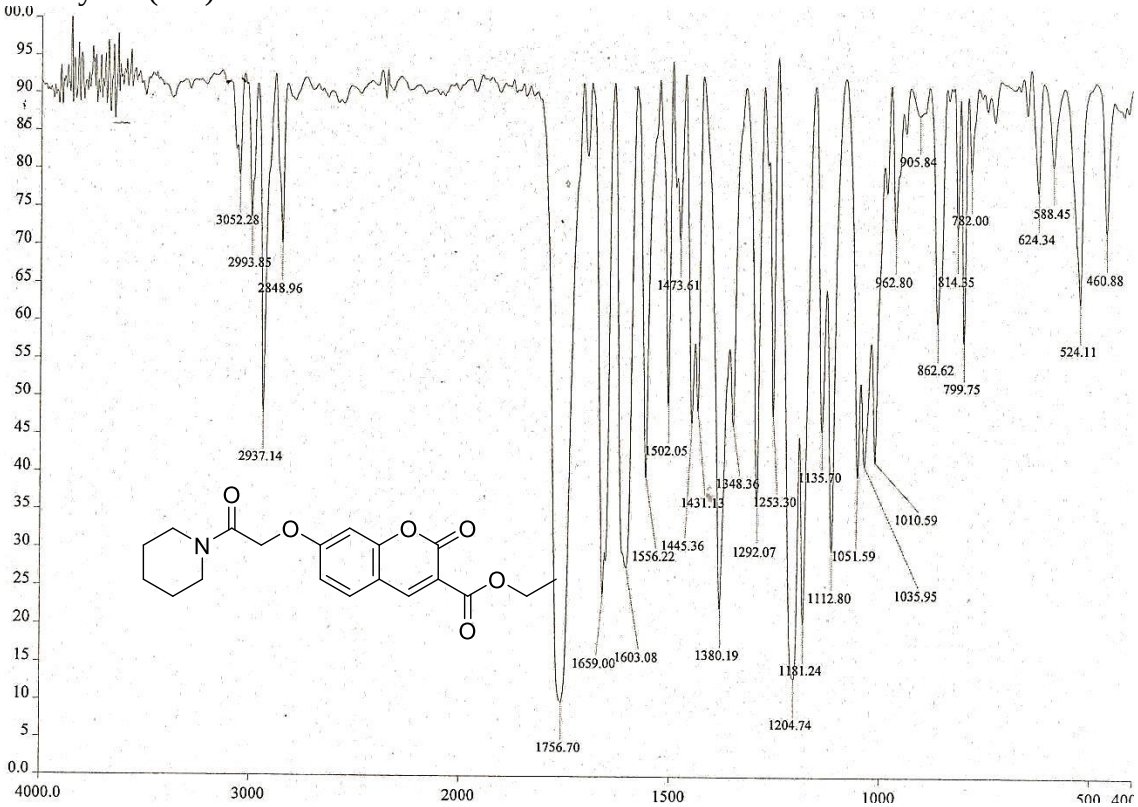

Figure-2.14.2 ^{1}H-NMR spectrum of ethyl 2-oxo-7-[2-oxo-2-(piperidin-1-yl)ethoxy]-2H-chromene-3-carboxylate (**10c**) in DMSO-d_6

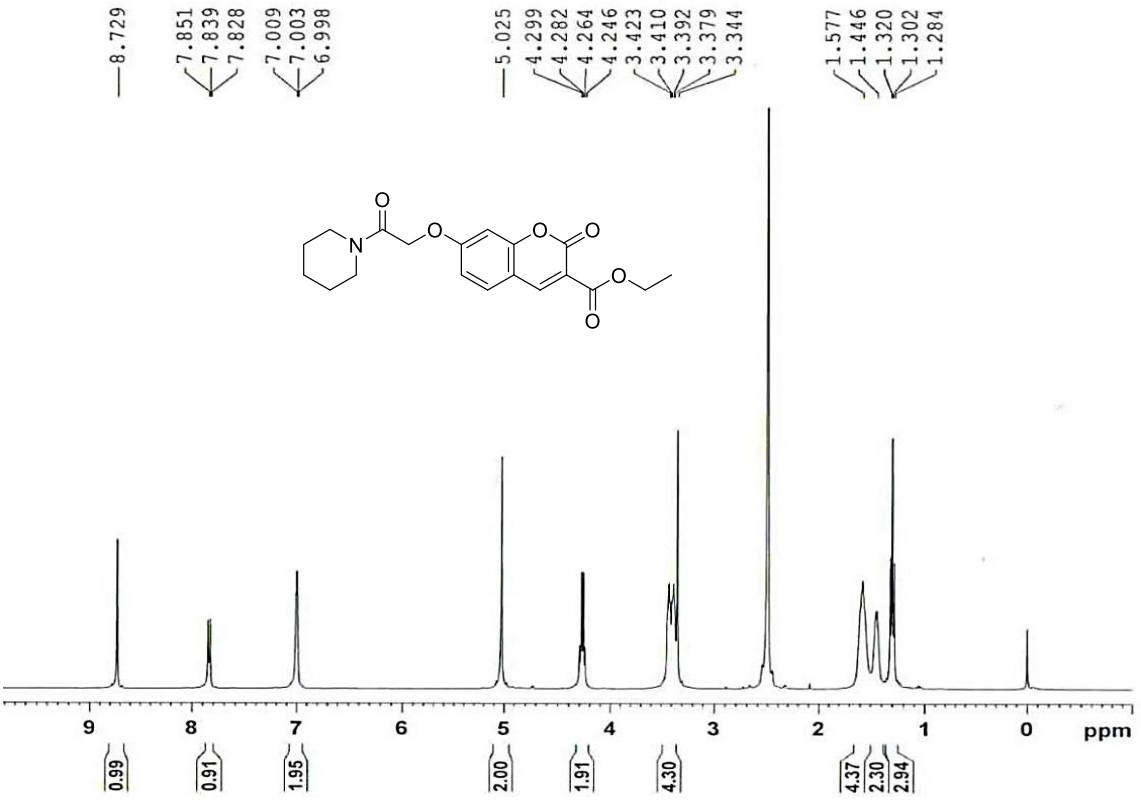

Figure-2.14.3 ^{13}C-NMR spectrum of ethyl 2-oxo-7-[2-oxo-2-(piperidin-1-yl)ethoxy]-2*H*-chromene-3-carboxylate (**10c**) in DMSO-d_6

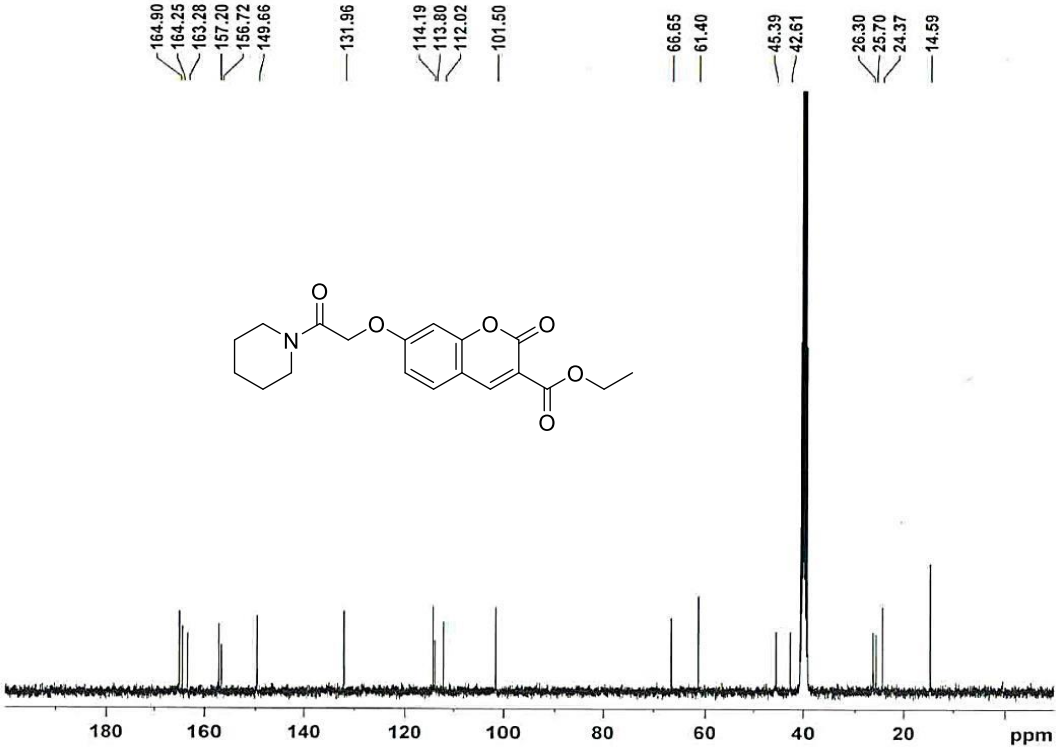

Figure-2.15.1 IR spectrum of ethyl 7-[2-(morpholin-4-yl)-2-oxoethoxy]-2-oxo-2H-chromene-3-carboxylate (**10d**)

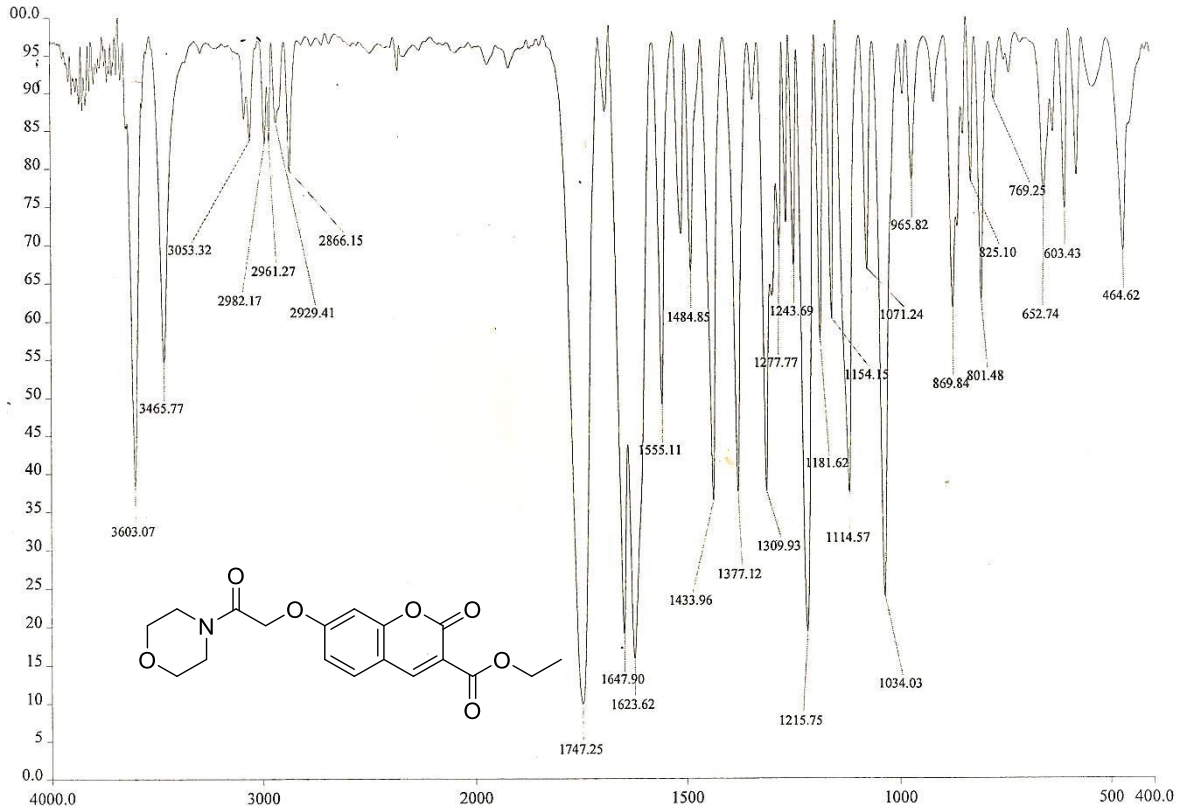

Figure-2.15.2 ^{1}H-NMR spectrum of ethyl 7-[2-(morpholin-4-yl)-2-oxoethoxy]-2-oxo-2H-chromene-3-carboxylate (**10d**) in $CDCl_3$

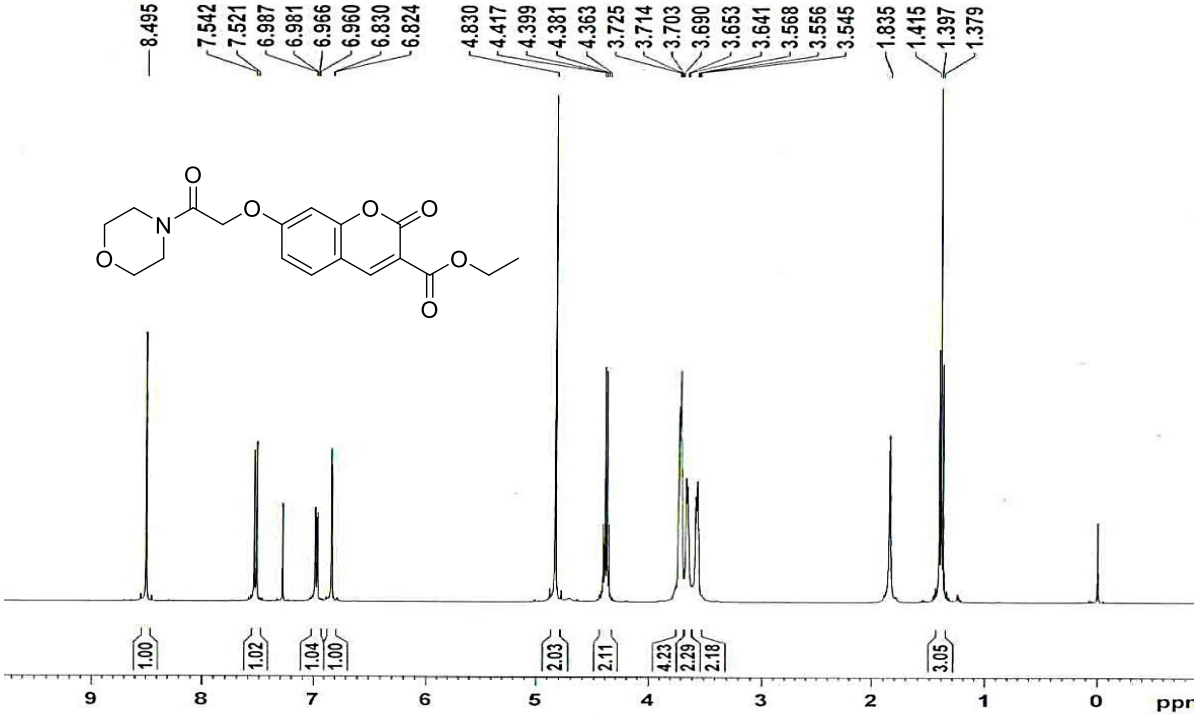

Figure-2.15.3 ^{13}C-NMR spectrum of ethyl 7-[2-(morpholin-4-yl)-2-oxoethoxy]-2-oxo-2H-chromene-3-carboxylate (**10d**) in $CDCl_3$

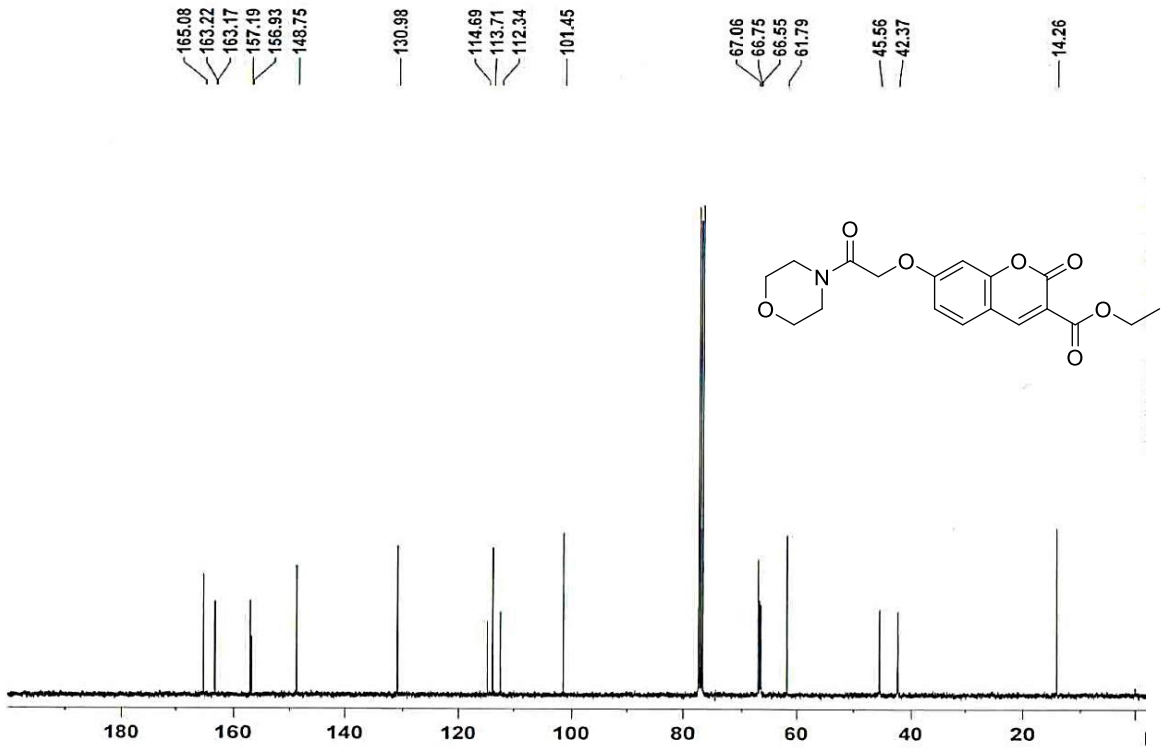

Figure-2.15.4 ESI-MS spectrum of ethyl 7-[2-(morpholin-4-yl)-2-oxoethoxy]-2-oxo-2*H*-chromene-3-carboxylate (**10d**) M+H peak at 362.05

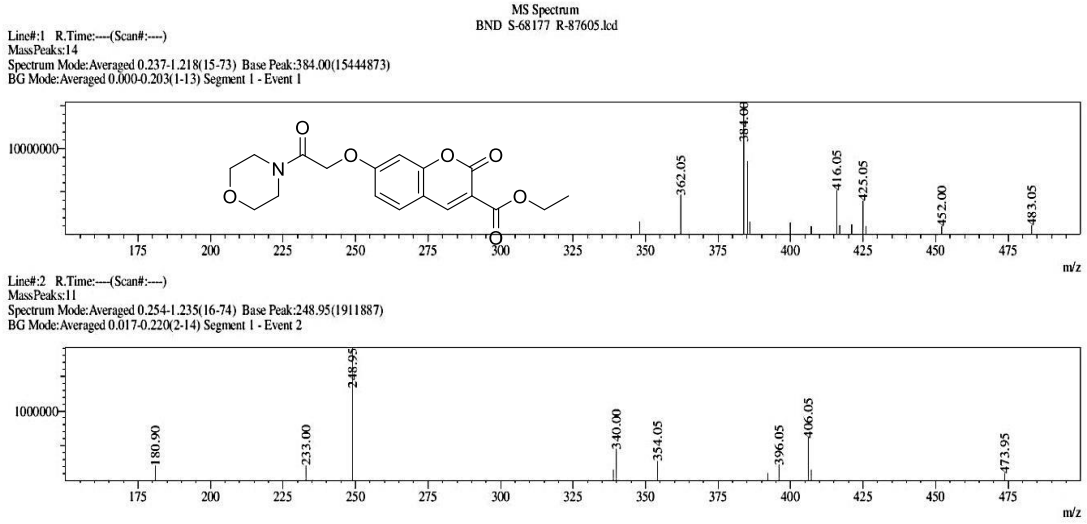

2.2.2 Biological Evaluation

Results from MTT assay were used to assess the growth inhibitory effect of the various compounds on A549 cancer cells (Lungs cancer cell line) and MCF7 (Breast cancer cell line). IC_{50} values were calculated to determine the concentration of test compound at which 50% of the cells are killed (Table-2.2). Compounds were studied for their DNA binding interaction (Table-2.3) and for their anti-oxidant activity against DPPH assay with respect to ascorbic acid as standard (Table-2.4).

2.2.3 Structure activity relationship (SAR) for anticancer activity

The MTT assay for 7-substituted-3-acetyl chromen-2-one series showed better activity for compound **8a** with *p*-methyl substituent on aromatic amide against A549 and MCF7 with IC_{50} 2.40 μM and 0.65 μM respectively. On replacement of p-methyl with halogen such as compounds **8b** and **8c** resulted in compounds with excellent activity (**Table-2.2**). Compound **8b** with 4-fluoro substituent showed excellent activity with IC_{50} value 0.16 nM against A549 cell line, and showed good activity against MCF7 cell line with IC_{50} 23.53 μM. Moreover, compound **8c** with 4-chloro showed very good activity with IC_{50} value 0.82 μM and 13.02 μM against A549 and MCF7 cancer cell lines respectively. Interestingly, changing position of halogen from *-para* to *-meta* in compound **8d** and **8e** resulted in drop of anticancer activity against A549 cell line. Compound **8d** with 3-fluoro group showed moderate activity with IC_{50} value 9.16 μM and 14.04 μM, but compound **8e** showed very good anticancer activity against MCF7 cell line with IC_{50} 84.8 nM, while moderate anticancer activity observed against A549

cell line. Further, replacement of aromatic ring with saturated nitrogen heterocycles such as pyrrolidine **8f** and piperidine **8g** resulted in compounds with moderate to very good activity against A549 cell line with IC_{50} value 23.9 µM and 5.06 µM respectively. Against MCF7 cell line both compounds **8f** and **8g** showed good activity with IC_{50} value 3.08 µM and 1.11 µM respectively. Compounds **8a**-**8c**, **8g** and **10b** showed better anticancer activity in A549, while compounds **8a-g** and **10a-d** showed better activity in MCF7 compared to that of 5-Fluorouracil. Compound **10a-10d** containing carboxylate group at third position of chromen-2-one ring showed good to poor anticancer activity, compared to corresponding 3-acetyl chromen-2-one analogues. Compound **10a** showed good activity against MCF7 cell line with IC_{50} 1.78 µM, however remain inactive against A549 cell line (**Table-2.2**).

Table-2.2 Anticancer activity against A549 (Lungs cancer cell line), MCF7 (Breast cancer cell line) and anti-oxidant activity of compound 8a-g and 10a-d.

Compd no.	NR^1R^2	R^3	A549 IC_{50}[a]	MCF7 IC_{50}[a]
8a	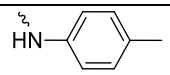	$-CH_3$	2.40 µM	0.65 µM
8b	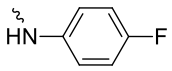	$-CH_3$	0.16 nM	23.53 µM
8c	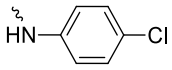	$-CH_3$	0.82 µM	13.02 µM
8d	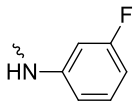	$-CH_3$	9.16 µM	14.04 µM
8e	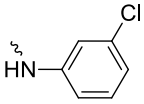	$-CH_3$	89.16 µM	84.8 nM
8f	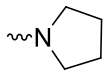	$-CH_3$	23.9 µM	3.08 µM
8g	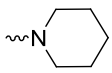	$-CH_3$	5.06 µM	1.11 µM
10a	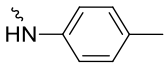	$-OC_2H_5$	NA	1.78 µM
10b	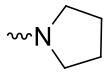	$-OC_2H_5$	3.11 µM	0.79 µM
10c	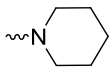	$-OC_2H_5$	NA	NA
10d	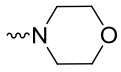	$-OC_2H_5$	23.2 µM	21.61 µM
5-Fluoro-uracil			11.13 µM	45.04 µM

[a]IC_{50} values were determined using Graph Pad Prism software by MTT assay using DMF.
NA = Not active

Carboxylate analogue of compound **8f** *i.e.* compound **10b** showed good activity against both tested cell lines A549 and MCF7 with IC_{50} 3.11 µM and 0.79 µM respectively. Compound

10c remained inactive against both tested cell lines. However, morpholine analogue compound **10d** showed good activity against A549 and MCF7 cell lines. 5-Fluorouracil was used as standard and showed anticancer activity with IC_{50} 45.04 µM against MCF7 cell line (**Table-2.2**).

2.2.4 DNA binding studies

Compounds **8b** and **8e** were selected for DNA-binding studies as they showed activity in nM concentration in MTT assay. For DNA binding UV based DNA titration and fluorescence emission study against DNA-EtBr complex were carried out as they provide more insight into mode of interaction of compounds with DNA [9, 20-21]. UV absorption titrations for compounds **8b** and **8e** were performed with tris-HCl buffer (pH 7.2). The fixed concentration of compounds **8b** and **8e** were titrated against the known concentration of CT-DNA solution. Both the compounds **8b** and **8e** showed good hypochromism shift (**Fig-2.16a,b**).

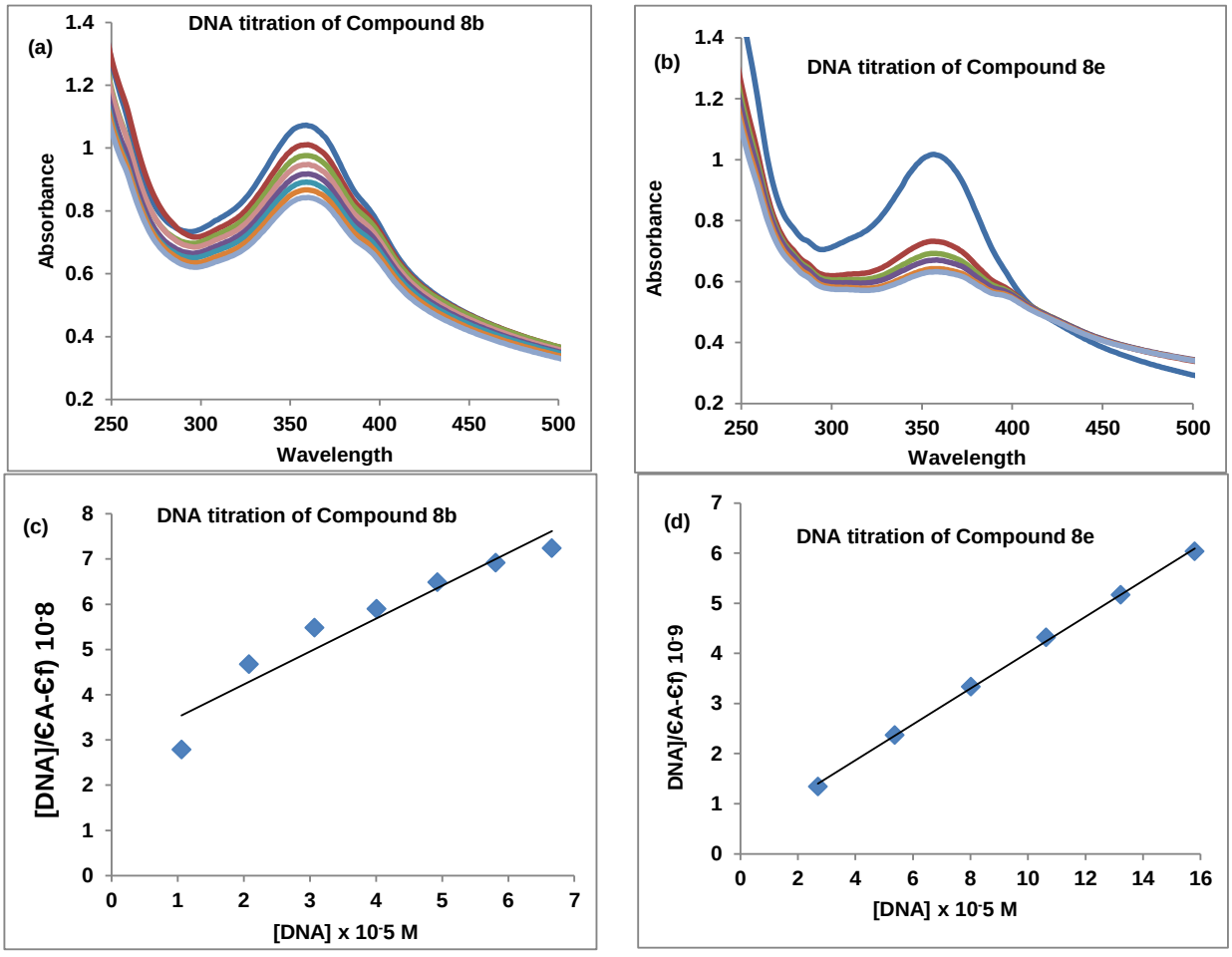

Figure-2.16: Titration plot of compounds **8b** and **8e** with DNA. Plot of Absorbance *versus* Wavelength nm for compound **8b** (a) and compound **8e** (b), Plot of $[DNA]/(Є_A-Є_f)$ versus [DNA] for compound **8b** (c) and compound **8e** (d).

The strength of binding to CT-DNA was determined through the calculation of intrinsic binding constant K_b which is obtained by monitoring the changes in the absorbance of the compounds with increasing concentration of CT-DNA. Plot of [DNA]/ (ε_A-ε_f) *versus* [DNA] (equation 1) is used to find out K_b. (**Fig-2.16c,d**).

$$[DNA]/ (\varepsilon_A-\varepsilon_f) = [DNA]/ (\varepsilon_b-\varepsilon_f) + 1/K_b(\varepsilon_b-\varepsilon_f) \quad \text{(eq 1)}$$

Where [DNA] is the concentration of DNA, $\varepsilon_A = A_{observed}/[compound]$, ε_f is the extinction coefficient for unbound compound and ε_b is the extinction coefficient for the compound in the fully bound form. In plot of [DNA]/ (ε_A-ε_f) *versus* [DNA], slope is equal to $1/(\varepsilon_b-\varepsilon_f)$ and Y-intercept is equal to $1/K_b(\varepsilon_b-\varepsilon_f)$. K_b is obtained from the ratio of slope to the Y-intercept (**Fig-2.16c,d**).

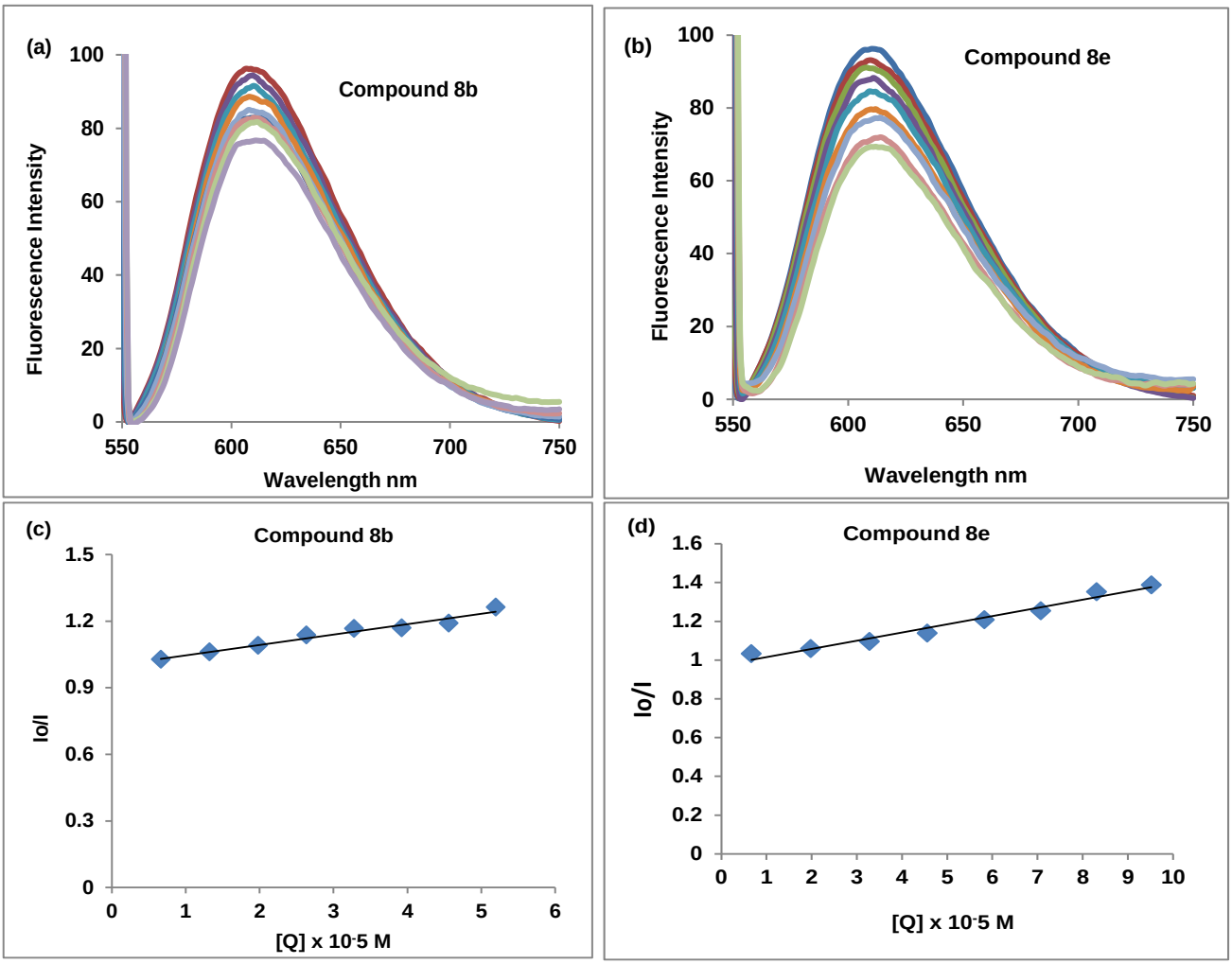

Figure-2.17: Plot of Fluorescence emission intensity I *versus* Wavelength (nm) for DNA-EtBr complex at different concentrations of compound **8b** (a) and compound **8e** (b), Stem-Volmer quenching Plot of DNA-EtBr for compound **8b** (c) and compound **8e** (d).

Compounds **8b** and **8e** showed the hypocromism shift with the intrinsic binding values 2.64 x 10^4 and 8.29 x 10^5 M^{-1} respectively in UV based DNA titrations which are indicative of DNA intercalative mode of binding (**Table-2.3**). To further confirm the mode of interaction of compounds **8b** and **8e** with DNA, fluorescence emmission based Ethidium bromide (EtBr) displacement assay was carried out. The emission spectra of DNA-EtBr (λ_{ex} =546 nm) in the absence and presence of increasing amount of compounds were recorded (**Fig-2.17a,b**).

The data were plotted according to the Stern-Volmer equation (equation 2) where I_0 and I are the flurosence intensities in the absence and presence of compound.

$$I_0/I = 1 + K_{SV}[Q] \qquad \text{(eq 2)}$$

Ksv is the Stern-Volmer quenching constant which can be obtained from the slope of straight line in plot of I_0/I *versus* [Q]. Quenching of fluoroscence intensity was observed for compounds **8b** and **8e** with Ksv 4.69 x 10^3 and 4.23 x 10^3 M^{-1} respectively which supports the DNA intercalating property of these compounds (**Table-2.3**, **Fig-2.17c,d**).

Table-2.3: K_b and K_{SV} values for compound **8b** and **8e**.

Compd	λ_{max} nm	K_b (M^{-1}) UV based assay	Emission λ_{max} Nm	K_{SV} (M^{-1}) Fluorescence assay
8b	359	2.64 x 10^4	609	4.69 x 10^3
8e	356	8.29 x 10^5	610	4.23 x 10^3

2.2.5 Antioxidant activity

The drug which showed good anticancer activity have poor antioxidant activity which give emphasis that the anticancer activity was may be due to reactive oxygen species.[22] Antioxidant activity of these entire synthesized compounds was screened by DPPH assay. Compounds which showed very good anticancer activity were found to be poor for antioxidant activity. Compounds **8a**-**8b** showed very poor antioxidant activity as compared to ascorbic acid (**Table-2.4**). Compounds **8d** and **8e** showed moderate anti-oxidant activity with EC_{50} 48 µg/mL and 59 µg/mL respectively. Interestingly, 3-carboxylate chromen-2-one compounds **10b** and **10c** showed good antioxidant activity with EC_{50} 46 and 47 µg/mL respectively. Compounds **8d**-**8e** and **10b**-**10c** showed scavenging activity similar to ascorbic acid at 100 µM concentration. Compounds **8c**, **8f**, **8g**, **10a** and **10d** remained inactive as antioxidant agent in DPPH assay.

Table-2.4 Anti-oxidant activity of compounds **8a-e** and **10b-c**.

Compound No.	EC_{50} µg/mL[a]
8a	3436
8b	882
8d	48
8e	59
10b	46
10c	47
Ascorbic acid	11

[a]EC_{50} values were determined using Graph Pad Prism software by DPPH assay using DMF.

2.3 Conclusion

New 3,7-disubstituted Chromen-2-one derivatives were synthesized to develop more potent anticancer or antioxidant agents. Screening of compound **8a-g** and **10a-d** was done and from the structure activity relationship study Compounds **8a-8c**, **8g** and **10b** showed good anticancer activity in A549 Lungs cancer cell line, while compounds **8a-g** and **10a,b** showed better activity in MCF7 Breast cancer cell line compared to that of 5-Fluorouracil.

Out of all screened compounds, **8b** showed IC_{50} value of 0.16nM in lung cancer cell line and compound **8e** exhibited IC_{50} value of 84.8nM in breast cancer cell line, both falling in nanomolar range which was very low concentration as compared to 5-Fluorouracil. Both compounds **8b** and **8e** showed binding mode through intercalation with DNA. The DNA interaction of compound **8e** was found to be very good with intrinsic binding constant 8.29 x 10^5 M^{-1} compared to that of compound **8b** 2.64 x 10^4 M^{-1} in UV based DNA titration. Both compounds showed good interaction with DNA by displacement of EtBr in DNA-EtBr complex by quenching its fluoresence. Antioxidant activity of selected synthesized compounds was done by DPPH assay. All compounds showed very poor antioxidant activity. Further analysis is going on to confirm this finding that most of these derivatives also causing apoptosis in cancer cell line *via* p53 mediated induction of reactive oxygen species.

2.4 Experimental

2.4.1 Chemistry

Reagent grade chemicals and solvents were purchased from commercial supplier and used after purification. TLC was performed on silica gel F254 plates (Merck). Acme's silica gel (60-120 mesh) was used for column chromatographic purification. All reactions were carried out in nitrogen atmosphere. Melting points are uncorrected and were measured in open capillary tubes, using a Rolex melting point apparatus. IR spectra were recorded as KBr pellets on Perkin Elmer RX 1 spectrometer. ^{1}H-NMR and ^{13}C-NMR spectral data were recorded on Advance Bruker 400 spectrometer (400 MHz) with $CDCl_3$ or DMSO-d_6 as solvent and TMS as internal standard. *J* values are in Hz. Mass spectra were determined by ESI-MS, using a Shimadzu LCMS 2020 apparatus. C,H,N analysis of all compounds were done to check the purity of compounds.

Preparation of 2,4 dihydroxy benzaldehyde (resorcaldehyde) (5)

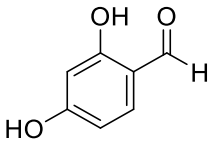

To an ice-cold solution of Resorcinol (12.5 mmol) in N,N-dimethylformamide (DMF) (8 mL) was added $POCl_3$ (12.7 mmol) dropwise at 0-5^{o}C with constant stirring over a period of 10 min. semi solid mass was stirred for 30 min at room temperature, white solid obtained was kept overnight and dissolved in 50% sodium acetate solution. The resulting solution was kept for overnight at 0-5^{o}C which on filtration gave light pink crystals of 2,4 dihydroxy benzaldehyde. M.P: 134-136 ^{o}C

Preparation of N-substituted chloroacetamide derivatives (7)

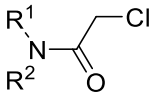

To an ice-cold solution of substituted amines (20 mmol) in dichloromethane (DCM) (25 mL) was added triethylamine (TEA) (20.2 mmol) and stirred for 5-10 min. To this chloroacetyl chloride (20 mmol) was added dropwise over a period of 10 min under cooling. The resulting solution was stirred at 0-5 ^{o}C for 30 min and at room temperature for 24 hrs. The reaction mixture was diluted with water and extracted with DCM (2 x 30 mL). The organic layer were combined, washed with HCl solution (0.5 N, 15 mL), dried over anhydrous Na_2SO_4, filtered and evaporated on a rotavapor to give compound **7**. The substituted chloroacetamide **7** thus obtained, used directly for next step without any purification.

Preparation of 3-acetyl-7-hydroxy-2H-chromen-2-one (6)

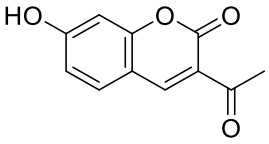

To a solution of 2,4-dihydroxy benzaldehyde (10.0 g, 72.463 mmol) and ethyl acetoacetate (9.16 mL, 72.463 mmol, 1.0 eq) in pyridine (20 mL) was added, catalytic amount of piperidine (0.5 mL). The resulting solution was stirred in bulb oven (100 W) at 70-80 ºC for 14 hrs. The reaction mixture was poured into mixture of crushed ice and Conc. HCl. The solid separated out was filtered, washed with water, dried and recrystallized from ethanol to obtained compound **6** as brown solid. Yield : 87%; M.P : 238 ºC (Lit M.P. 240 ºC [23]); ^{1}H-NMR (400 MHz, DMSO-d_6): 2.53 (s, 3H), 6.72 (d, *J*=2.0, 1H), 6.83 (dd, *J*=2.0, 8.8 1H), 7.76 (d, *J*=8.8 Hz, 1H), 8.56 (s, 1H), 11.14 (br s, 1H); ^{13}C-NMR (100 MHz, DMSO-d_6): 30.55, 102.19, 111.23, 114.65, 119.63, 133.14, 148.23, 157.69, 159.50, 164.61, 195.11.

Preparation of ethyl 7-hydroxy-2-oxo-2H-chromene-3-carboxylate (9)

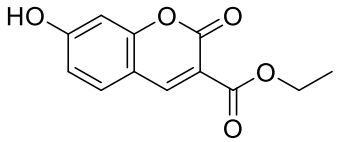

Compound **9** was prepared using method described for preparation of compound **6**, only diethyl malonate was used instead of ethyl acetoacetate. Compound **9** was obtained as white crystals after recrystallization from ethanol. Yield : 74 %; M.P : 164ºC (Lit M.P. 166 ºC [24]); ^{1}H-NMR (400 MHz, DMSO-d_6): 1.29 (t, *J*=7.2 Hz, 3H), 4.26 (q, *J*=7.2 Hz, 2H), 6.72 (d, *J*=2.0 Hz, 1H), 6.84 (dd, *J*=2.0,8.8 Hz, 1H), 7.76 (d, *J*=8.8 Hz, 1H), 8.67 (s, 1H), 11.10 (br s, 1H) ; ^{13}C-NMR (100 MHz, DMSO-d_6): 14.60, 61.27, 102.24, 110.88, 112.52, 114.46, 132.58, 149.93, 156.86, 157.56, 163.40, 164.52.

General procedure for the synthesis of compounds 8a-g** and **10a-d

To a solution of compound **6**/ **9** (1.0 eq) in dry *N*,*N*-dimethylformamaide (DMF) (15 mL) was added compound **7** (1.2 eq). To this anhydrous K_2CO_3 (1.5 eq) was added followed by pinch of KI. The resulting mixture was heated in water bath at 70-80 ºC 12-18 hrs. The completion of reaction was checked by TLC using pet. ether: ethyl acetate (1:1). The reaction mixture was poured in ice cold water. The solid separated out was filtered, washed with water and dried. When there was no solid separated out in water, the aqueous layer was extracted using DCM (3 x 20 mL). The organic layers were combined, washed with brine, dried over anhydrous Na_2SO_4, filtered and concentrated to give an oily residue. The residue was

triturated in pet. ether to give compound as solid. The crude compound was purified by column chromatography over silica gel using pet. ether: ethyl acetate (40:60 to 20:80) to obtained pure compound as solid.

Characterization data for compounds 8a-g and 10a-d

2-[(3-Acetyl-2-oxo-2H-chromen-7-yl)oxy]-N-(4-methylphenyl)acetamide (8a)

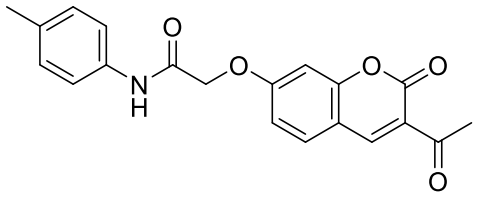

Pale yellow solid, Yield: 91 %; M.P: 212 ºC; IR (KBr): 3374, 3053, 2919, 1727, 1681, 1613, 1597, 1372, 1204, 1052, 820, 770 cm^{-1}; ^{1}H-NMR (400 MHz, $CDCl_3$): δ 2.35 (s, 3H), 2.73 (s, 3H), 4.72 (s, 2H), 6.96 (d, *J*=2.2 Hz, 1H), 7.04 (dd, *J*=2.2, 8.8 Hz, 1H), 7.19 (d, *J*=8.4 Hz, 2H), 7.48 (d, *J*=8.4 Hz, 2H), 7.66 (d, *J*=8.8 Hz, 1H), 8.10 (s, 1H), 8.52 (s, 1H); ^{13}C-NMR (100 MHz, $CDCl_3$): δ ppm 20.95, 30.62, 67.71, 102.04, 113.29, 113.33, 120.35, 121.92, 129.71, 132.03, 133.84, 135.06, 147.31, 157.37, 159.27, 161.86, 164.37, 195.34; Anal. Calc. for $C_{20}H_{14}NO_5$; C, 68.37; H, 4.88; N, 3.99; found: C, 68.22; H, 4.90; N, 3.72 %; ESI-MS: 352.0 $[M+H]^+$.

2-[(3-Acetyl-2-oxo-2H-chromen-7-yl)oxy]-N-(4-fluorophenyl)acetamide (8b)

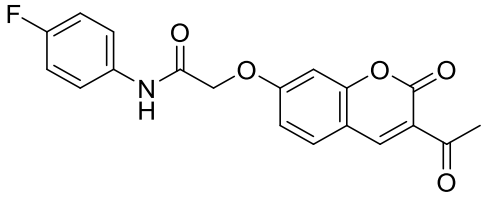

Yellow solid, Yield: 86 %; M.P: 222 ºC; IR (KBr): 3374, 3112, 1728, 1687, 1611, 1596, 1551, 1542, 1455, 1374, 1363, 1262, 1202, 1128, 1956, 838, 769 cm^{-1}; ^{1}H-NMR (400 MHz, DMSO-d_6): δ 2.56 (s, 3H), 4.89 (s, 2H), 7.09-7.12 (m, 2H), 7.15-7.19 (m, 2H), 7.62-7.66 (m, 2H), 7.91 (d, *J*=8.8 Hz, 1H), 8.64 (s, 1H), 10.25 (s, 1H); ^{13}C-NMR (100 MHz, DMSO-d_6): δ ppm 30.55, 67.75, 101.60, 112.74, 114.19, 115.74, 115.96, 121.22, 121.95, 122.02, 132.70, 135.08, 135.10, 147.96, 157.25, 159.27, 163.69, 165.97, 195.25; Anal. Calc. for $C_{19}H_{14}FNO_5$; C, 64.23; H, 3.97; N, 3.94; found: C, 63.98; H, 3.75; N, 3.69 %; ESI-MS: 356.0 $[M+H]^+$.

2-[(3-Acetyl-2-oxo-2H-chromen-7-yl)oxy]-N-(4-chlorophenyl)acetamide (8c)

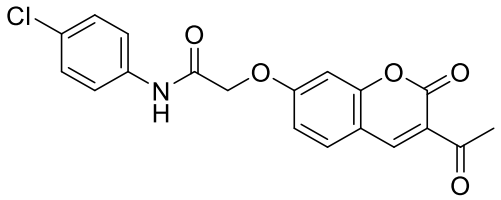

Pale yellow solid, Yield: 79 %; M.P: 218 ºC; IR (KBr): 3364, 2925, 2355, 1728, 1682, 1615, 1593, 1531, 1454, 1372, 1260, 1203, 1127, 1056, 1010, 831, 770 cm^{-1}; ^{1}H-NMR (400 MHz, DMSO-d_6): δ 2.56 (s, 3H), 4.91 (s, 2H), 7.10-7.12 (m, 2H), 7.38 (d, *J*=6.8 Hz, 2H), 7.64 (d, *J*=9.2 Hz, 2H), 7.91 (d, *J*= 9.2 Hz, 1H), 8.64 (s, 1H), 10.33 (s, 1H); ^{13}C-NMR (100 MHz, DMSO-d_6): δ ppm 30.55, 67.75, 101.60, 112.75, 114.19, 121.23, 121.65, 127.83, 129.18, 132.70, 137.71, 147.95, 157.25, 159.27, 163.68, 166.21, 195.25; Anal. Calc. for $C_{19}H_{14}ClNO_5$; C, 61.38; H, 3.80; N, 3.77; found: C, 61.16; H, 4.02; N, 3.94 %; ESI-MS: 394.00 $(M+Na)^+$.

2-[(3-Acetyl-2-oxo-2H-chromen-7-yl)oxy]-N-(3-fluorophenyl)acetamide (8d)

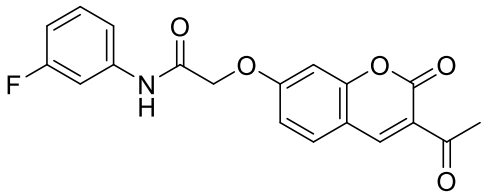

Yellow solid, Yield: 81 %; M.P: 236 ºC; IR(KBr): 3411, 3073, 3047, 2930, 2360, 1734, 1698, 1670, 1616, 1538, 1506, 1450, 1435, 1375, 1359, 1259, 1216, 1134, 1051, 978, 769, 674 cm^{-1}; ^{1}H-NMR (400 MHz, DMSO-d_6): δ 2.60 (s, 3H), 4.92 (s, 2H), 6.90-6.93 (m, 1H), 7.09-7.11 (m, 2H), 7.34-7.37 (m, 2H), 7.60 (d, *J*=11.2 Hz, 1H), 7.91 (d, *J*=9.2 Hz, 1H), 8.64 (s, 1H), 10.41 (s, 1H); ^{13}C-NMR (100 MHz, DMSO-d_6): δ ppm 30.54, 67.79, 101.61, 106.97, 110.82, 112.76, 114.17, 115.81, 121.24, 131.00, 132.70, 140.52, 147.94, 157.25, 159.26, 161.34, 163.74, 166.43, 195.23; Anal. Calc. for $C_{19}H_{14}FNO_5$; C, 64.23; H, 3.97; N, 3.94; found: C, 63.98; H, 3.90; N, 3.76 %; ESI-MS: 356.0 $[M+H]^+$.

2-[(3-Acetyl-2-oxo-2H-chromen-7-yl)oxy]-N-(3-chlorophenyl)acetamide (8e)

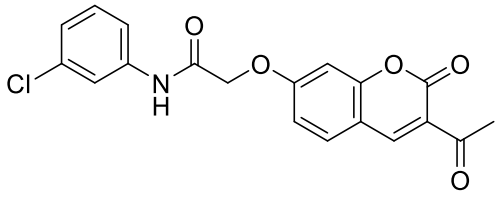

Pale yellow solid, Yield: 73 %; M.P: 210 ºC; IR (KBr): 3403, 3107, 3056, 1727, 1697, 1621, 1428, 1373, 1211, 770 cm^{-1}; ^{1}H-NMR (400 MHz, DMSO-d_6): δ 2.55 (s, 3H), 4.91 (s, 2H),

7.08-7.15 (m, 3H), 7.35 (t, *J*=8.0 Hz, 1H), 7.51(d, *J*=8.4 Hz, 1H), 7.81 (s, 1H), 7.88 (d, *J*=8.4 Hz, 1H), 8.62 (s, 1H), 10.38 (s, 1H); ^{13}C-NMR (100 MHz, DMSO-d_6): δ ppm 30.52, 67.68, 101.61, 112.74, 114.15, 118.47, 119.55, 121.19, 123.96, 130.96, 132.68, 133.54, 140.16, 147.92, 157.23, 159.24, 163.62, 166.45, 195.21; Anal. Calc. for $C_{19}H_{14}ClNO_5$; C, 61.38; H, 3.80; N, 3.77; found: C, 61.18; H, 3.37; N, 3.49 %; ESI-MS: 393.99 $(M+Na)^+$.

3-Acetyl-7-[2-oxo-2-(pyrrolidin-1-yl)ethoxy]-2H-chromen-2-one (8f)

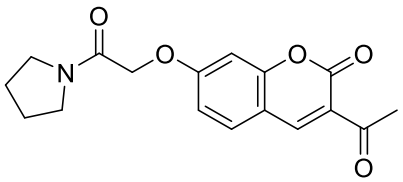

Pale yellow solid, Yield: 54 %; M.P: 146 ºC; IR (KBr): 3025, 2995, 2966, 2883, 1745, 1689, 1667, 1614, 1590, 1548, 1510, 1457, 1424, 1357, 1307, 1213, 1177, 1145, 1041, 989, 852, 804, 770, 744 cm^{-1}; ^{1}H-NMR (400 MHz, $CDCl_3$): δ 1.87-1.94 (m, 2H), 2.01-2.08 (m, 2H), 2.70 (s, 3H), 3.49-3.57 (m, 4H), 4.75 (s, 2H), 6.82 (d, *J*=2.4 Hz, 1H), 6.99 (dd, *J*=2.4, 8.8 Hz, 1H), 7.57 (d, *J*=8.8 Hz, 1H), 8.49 (s, 1H); ^{13}C-NMR (100 MHz, $CDCl_3$): δ ppm 23.83, 26.24, 30.58, 45.74, 46.29, 67.33, 101.27, 112.60, 114.11, 121.05, 131.65, 147.67, 157.46, 159.60, 163.62, 164.75, 195.46; Anal. Calc. for $C_{17}H_{17}NO_5$; C, 64.75; H, 5.43; N, 4.44; found: C, 64.30; H, 5.23; N, 4.19 %; ESI-MS: 316.0 $(M+H)^+$.

3-Acetyl-7-[2-oxo-2-(piperidin-1-yl)ethoxy]-2H-chromen-2-one (8g)

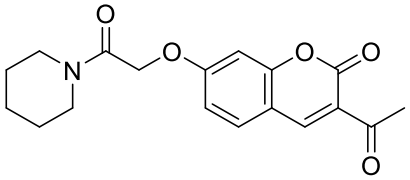

Yellow solid, Yield: 51 %; M.P: 118 ºC; IR (KBr): 2935, 2856, 1723, 1683, 1662, 1614, 1594, 1551, 1504, 1435, 1366, 1252, 1231, 1214, 1167, 1150, 1137, 1064, 1012, 984, 955, 841, 771 cm^{-1}; ^{1}H-NMR (400 MHz, $CDCl_3$): δ 1.56-1.69 (m, 6H), 2.69 (s, 3H), 3.44 (t, *J*=5.2 Hz, 2H), 3.56 (t, *J*=5.2 Hz, 2H), 4.82 (s, 2H), 6.83 (d, *J*=2.2 Hz, 1H), 6.97 (dd, *J*=2.2, 8.6 Hz, 1H), 7.55 (d, *J*=8.6 Hz, 1H), 8.47 (s, 1H); ^{13}C-NMR (100 MHz, $CDCl_3$): δ ppm 24.32, 25.45, 26.48, 30.56, 43.27, 46.15, 67.19, 101.41, 112.58, 113.93, 121.04, 131.67, 147.63, 157.44, 159.57, 163.63, 164.46, 195.44; Anal. Calc. for $C_{18}H_{19}NO_5$; C, 65.64; H, 5.82; N, 4.25; found: C, 65.40; H, 5.90; N, 4.05 %; ESI-MS: 330.0 $[M+H]^+$.

Ethyl 7-{2-[(4-methylphenyl)amino]-2-oxoethoxy}-2-oxo-2H-chromene-3-carboxylate (10a)

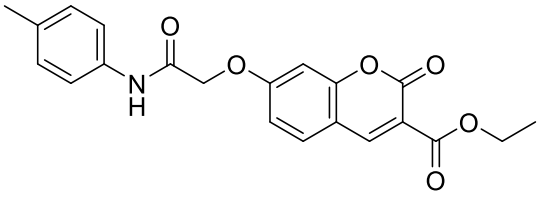

Yellow solid, Yield : 84 %; M.P : 178 ºC; IR (KBr): 3344, 3085, 3035, 2983, 2915, 1757, 1708, 1605, 1547, 1506, 1437, 1384, 1296, 1207, 1049, 963, 811, 665 cm^{-1}; ^{1}H-NMR (400 MHz, $CDCl_3$): 1.42 (t, *J*=7.2 Hz, 3H), 2.35 (s, 3H), 4.42 (q, *J*=7.2 Hz, 2H), 4.71 (s, 2H), 6.94 (d, *J*=2.0 Hz, 1H), 7.02 (dd, *J*=2.4, 8.8 Hz, 1H), 7.18 (d, *J*=8.4 Hz, 2H), 7.48 (d, *J*=8.4 Hz, 2H), 7.61 (d, *J*=8.8 Hz, 1H), 8.15 (s, 1H), 8.52 (s, 1H); ^{13}C-NMR (100 MHz, $CDCl_3$): 14.27, 20.94, 61.93, 67.71, 102.23, 112.92, 112.98, 115.52, 120.37, 129.68, 131.24, 133.91, 134.99, 148.46, 156.68, 157.16, 161.84, 163.18, 164.46; Anal. Calc. for $C_{21}H_{19}NO_6$; C, 66.14; H, 5.02; N, 3.67; found: C, 66.28; H, 5.16; N, 3.67 %; ESI-MS: 382.0$[M+H]^+$.

Ethyl 2-oxo-7-[2-oxo-2-(pyrrolidin-1-yl)ethoxy]-2H-chromene-3-carboxylate (10b)

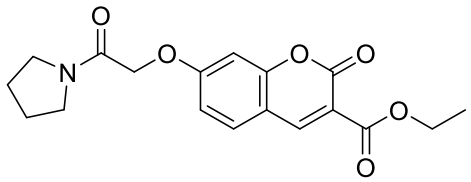

Off white solid, Yield : 48 %; M.P : 144 ºC; IR (KBr): 3077, 3047, 2979, 1756, 1659, 1602, 1556, 1500, 1440, 1379, 1280, 1208, 1185, 1113, 1039, 1000, 871, 824, 801, 629 cm^{-1}; ^{1}H-NMR (400 MHz, DMSO-d_6): 1.30 (t, *J*=6.8 Hz, 3H), 1.76-1.79 (m, 2H), 1.89-1.92 (m, 2H), 3.32-3.46 (m, 4H), 4.27 (q, *J*=6.8 Hz, 2H), 4.93 (s, 2H), 7.00 (s, 2H), 7.83 (d, *J*=8.8 Hz, 1H), 8.73 (s, 1H); ^{13}C-NMR (100 MHz, DMSO-d_6): 14.58, 23.99, 26.08, 44.92, 46.05, 61.40, 66.77, 101.49, 112.02, 113.77, 114.19, 131.94, 149.67, 156.72, 157.21, 163.28, 164.26, 165.06; Anal. Calc. for $C_{18}H_{19}NO_6$; C, 62.60; H, 5.55; N, 4.06; found: C, 62.47; H, 5.52; N, 3.98 %; ESI-MS: 346.05 $[M+H]^+$.

Ethyl 2-oxo-7-[2-oxo-2-(piperidin-1-yl)ethoxy]-2H-chromene-3-carboxylate (10c)

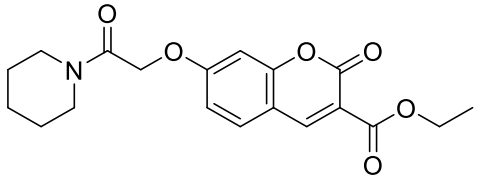

Off white solid, Yield : 43 %; M.P : 130 ºC; IR (KBr): 3052, 2993, 2937, 2848, 1756, 1659, 1603, 1556, 1502, 1445, 1431, 1380, 1292, 1204, 1181, 1112, 1051, 1035, 1010, 962, 862, 799 cm^{-1}; ^{1}H-NMR (400 MHz, DMSO-d_6): 1.30 (t, *J*=7.2 Hz, 3H), 1.44 (br s, 2H), 1.57 (br s,

4H), 3.34-3.42 (m, 4H), 4.27 (q, *J*=7.2 Hz, 2H), 5.02 (s, 2H), 6.99-7.00 (m, 2H), 7.82-7.85 (m, 1H), 8.73 (s, 1H); ^{13}C-NMR (100 MHz, DMSO-d_6): 14.59, 24.37, 25.70, 26.30, 42.61, 45.39, 61.40, 66.61, 101.50, 112.02, 113.80, 114.19, 131.96, 149.66, 156.72, 157.20, 163.28, 164.25, 164.90; Anal. Calc. for $C_{19}H_{21}NO_6$; C, 63.50; H, 5.89; N, 3.90; found: C, 63.23; H, 5.72; N, 3.63 %; ESI-MS: 360.0 $[M+H]^+$.

Ethyl 7-[2-(morpholin-4-yl)-2-oxoethoxy]-2-oxo-2H-chromene-3-carboxylate (10d)

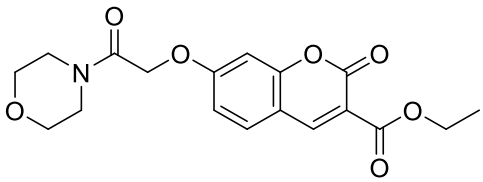

Pale green solid, Yield : 64 %; M.P : 124 ºC; IR (KBr): 3053, 2982, 2961, 2929, 2866, 1747, 1647, 1623, 1555, 1484, 1433, 1377, 1309, 1215, 1114, 1034, 965, 869, 801, 652 cm^{-1}; ^{1}H-NMR (400 MHz, $CDCl_3$): 1.39 (t, *J*=7.2 Hz, 3H), 3.54-3.56 (m, 2H), 3.64-3.65 (m, 2H), 3.69-3.72 (m, 4H), 4.39 (q, *J*=7.2 Hz, 2H), 4.83 (s, 2H), 6.83 (d, *J*=2.4 Hz, 1H), 6.97 (dd, *J*=2.4, 8.4 Hz, 1H), 7.53 (d, *J*=8.4 Hz, 1H), 8.49 (s, 1H) ; ^{13}C-NMR (100 MHz, $CDCl_3$): 14.26, 42.36, 45.56, 61.79, 66.55, 66.75, 67.06, 101.45, 112.34, 113.71, 114.69, 130.98, 148.75, 156.93, 157.19, 163.17, 163.22, 165.05; Anal. Calc.for $C_{18}H_{19}NO_7$; C, 59.83; H, 5.30; N, 3.88; found: C, 59.68; H, 5.52; N, 3.60 %; ESI-MS: 362.05 $(M+H)^+$.

2.4.2 Material and Methods for Biological evaluation

2.4.2.1 MTT Assay

The compounds were tested for their cytotoxic potential on two types of cancer cells, *viz.*, A549 (lung cancer cell-line) and MCF7 (breast cancer cell-line). The MTT assay was used to determine the effect of each compound on the proliferation of cancer cells. Fluorouracil (Neon Laboratory) was used as standard.

A549 and MCF7 cultures were purchased from National Centre for Cell Science, Pune, India. All growth media, supplements and reagents were purchased from HiMedia Labs, Mumbai, India. For the assay, cells were seeded at 10^5 cells/ml in a 96-well plate in dulbecco's modified minimum essential medium (DMEM) supplemented with 10% fetal bovine serum (FBS). To each well, test compound was added at six different concentrations of 100µM, 50µM, 10µM, 5µM, 1µM and 0.5µM. Each concentration was tested in triplicates. The cells were incubated with these compounds at 37^{o}C under 5% CO_2 for 48 hours. Following this, 3-[4,5-dimethylthiazol-2-yl]-2,5-diphenyltetrazolium bromide (MTT) was added to each well at a final concentration of 0.5mg/ml. Cells were incubated with this tetrazolium dye for 4 hours.

Subsequently, purple crystals of formazan were observed in each well, formed as a metabolic product of MTT. These crystals were dissolved in Isopropanol and the absorbance in each well was recorded at 570nm in a microplate reader (Metertech Sigma360). Absorbance at 570nm directly correlates with cell viability. IC_{50} (μM) values were determined using Graph Pad prism software.

2.4.2.2 UV-DNA binding assay

PerkinElmer Lambda- 35 dual beam UV–Vis spectrophotometer was used for absorption spectral studies. Solution of calf thymus DNA (CT DNA) was prepared in water. The UV absorbance at 260 was found to 0.358 which is used to calculate the DNA concentrations (ε = 6600 M^{-1}) and was expressed in terms of base molarity. UV absorption titrations were carried out by keeping the concentration of compounds **8b** to **8e** (dissolved in DMSO) fixed and by adding a known concentration of CT DNA solution in both the cuvettes in increasing amount until hypochromism saturation was observed. Absorbance values were recorded after each successive addition of DNA solution and equilibration.

2.4.2.3 Ethidium Bromide Displacement Assay

DNA (100 μL, 5.42 x 10^{-4} M), EtBr (100 μL, 2.71 x 10^{-4} M), and Tris-HCl buffer pH 7.2 was used to make a total volume of 3 mL EtBr displacement fluorescence assay was employed to find DNA intercalation. Fluoresence emission spectra (λmax= 600 nm, excitation wavelength 546nm, slit width 10nm, 1cm path length) were obtained at 30^{o}C on a JASCO FP-6300 fluorescence spectrophotometer. The assays were performed by using different concentrations of compound in buffer solution (3mL). I_0/I is plotted along with y axis against the concentration of compound, where in I and I_0 are the fluorescence intensities of the DNA-EtBr complex in the presence of and in the absence of compounds, respectively.

2.4.2.5 DPPH Assay

Free radical scavenging activity of different chromen-2-one derivatives were measured using 1,1-diphenyl-2-picryl hydrazyl (DPPH, Sigma). In brief, derivatives were added to 0.2 mM DPPH solution (100μl) at various concentrations (50, 100, 250, 450, 650, 850, 1000 μM) (100 μl) and incubated at 37^{0}C for 30 min in dark. The absorbance was measured at 490 nm in microplate reader (Metertech Sigma360). The control contains only DPPH solution in DMF while DMF served as blank (negative control) and ascorbic acid was taken as reference compound. Experiment was done in triplicate. The inhibition percentage (%) of radical scavenging activity was calculated as A_0 - A_1 / A_0X100. Where A_0 was the Absorbance of control reaction and A_1 was the Absorbance in presence of test or standard sample. Lower

absorbance of the reaction mixture indicated higher free radical activity. EC_{50} values were determined using Graph Pad prism software.

2.5 References

[1] Cancer fact sheet No-297, World Health Organisation (2015) Feb 2015.

[2] M. Mareel, A. Leroy, *Physiol. Rev.,* **2003**, *83*, 337.

[3] J. Wesche, K. Haglund, E. M. Haugsten, *Biochem. J.,* **2011**, *437*, 199.

[4] S. K. Grant, *Cell. Mol. Life Sci.,* **2009**, *66*, 1163.

[5] G. I. Solyanik, *Exp. Oncol.,* **2011**, *32*, 181.

[6] S. Vijayaraghavalu, C. Peetla, S. Lu, V. Labhasetwar, *Mol. Pharm.,* **2012**, *9*, 2730.

[7] H.-Y. Hung, E. Ohkoshi, M. Goto, K.F. Bastow, K. Nakagawa-Goto, K.-H. Lee, *J. Med. Chem.,* **2012**, *55*, 5413.

[8] S. Riedl, D. Zweytick, K. Lohner, *Chem. Phys. Lipids,* **2011**, *164*, 766.

[9] P. Bhattacharya, S. M. Mandal, A. Basak, *Eur. J. Org. Chem.,* **2016**, 1439.

[10] V. Sosa, T. Moliné, R. Somoza, R. Paciucci, H. Kondoh, M. E. Lleonart, *Ageing Res. Rev.,* **2013**,*12*, 376.

[11] S. Afzal, S. Jensen, J. Sørensen, T. Henriksen, A. Weimann, H. Poulsen, *Cancer Chemother. Pharmacol.,* **2012**, *69*, 301.

[12] J. Alexandre, Y. Hu, W. Lu, H. Pelicano, P. Huang, *Cancer Res.,* **2007,** *67*, 3512.

[13] D. Conley, E. M. Marshall, *Proc. Am. Assoc. Cancer Res.,* **1987**, *28*, 63.

[14] A. Thakur, R. Singla, V. Jaitak, *Eur. J. Med. Chem.,* **2015**, *101*, 476.

[15] Y. J. Li, C. Y, Wang, M. Y. Ye, G. Y. Yao, H. S. Wang, *Molecules,* **2015**, *20*, 14791.

[16] S. Emami, S. Dadashpour, *Eur. J. Med. Chem.,* **2015**, *102*, 611.

[17] J. T. Konc, E. Hejchman, H. Kruszewska, I. Wolska, D. Maciejewsk, *Eur. J. Med. Chem.,* **2011**, *46*, 2252.

[18] A. H. Halawa, A. A. E. Hassan, M. A. El-Nassag, M. M. A. El-All, G. E. El-Jaleel, E. M. Eliwa, A. H. Bedair, *Eur. J. Chem.,* **2014**, *5*, 111.

[19] Y. Wang, H. Liu, P. Lu, R. Mao, X. Xue, C. Fan, J. She, *Chem. Biol. Drug Des.,* **2015,** *8*6, 637.

[20] S. S. Mandal, U. Varshney, S. Bhattacharya, *Bioconjugate Chem*., **1997**, *8***,** 798.

[21] C. V. Kumar, E. H. Asunsion, *J. Am. Chem. Soc.,* **1993**, *115,* 8547.

[22] D. Dreher, A. F. Junod, *Eur. J. Cancer,* **1996**, *32,* 30.

[23] D. N. Shah, N. M. Shah, *J. Org. Chem.,* **1954**, *19***,** 1681.

[24] F. Bigi, L. Chesini, R. Maggi, G. Sartori, *J. Org. Chem.*, **1999**, *64*, 1033.